A Combined Computational, Experimental, and Technology Development Approach to In-Space Laser Manufacturing Maturation at NASA Marshall Space Flight Center

Andrew O'Connor, Jonathan M Bonebrake, Thomas C Bryan, Zachary S Courtright, Charles T Cowen, Ellis R Crabtree, William C Evans, Nathan Fripp, John C. Ivester, Emma K Jaynes, Louise S Littles, Christopher S Protz, Benjamin L Rupp, Jeffrey W Sowards

NASA Marshall Space Flight Center

Presented on 2024-12-05 at DMC24 in Austin, TX

In-space laser manufacturing enables space infrastructure

Method → ↓ Criteria	Fasteners/ rivets	In–Space Welding (ISW)
Joint strength & rigidity	◒	○
Joint hermeticity	●	○
Joint mass	●	○
Joint design & manufacturing simplicity	◒	○
Joint reliability	◒	○
Repair versatility	●	○
Associated cost & upmass	◒	○
● - Poor	◒ - Satisfactory	○ - Good

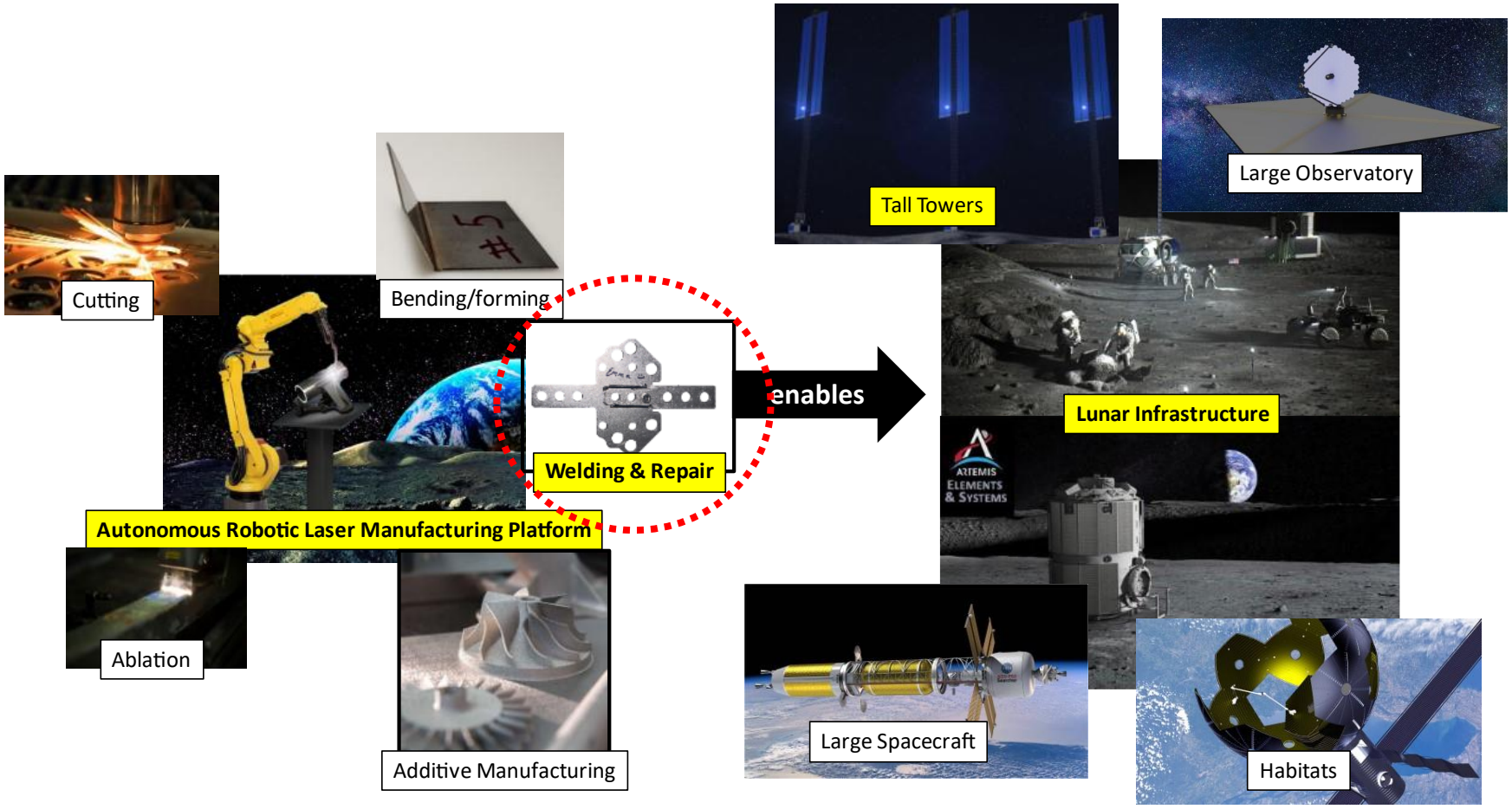

Image credit: ThinkOrbital, www.mechanicalcaveman.com

Timeline of In-Space Welding and Joining

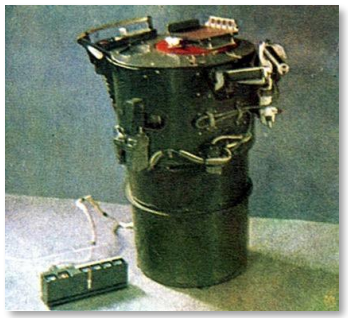

1960s | 1970s | 1980s | 1990s | 2000s | 2010s | 2020s

FIRST SPACE WELD 1969. Soyuz-6. Vulkan EBW, PAW, GMAW (USSR)

FIRST AMERICAN SPACE WELD 1973. Skylab. EBW, braze experiments (USA)

1979. Salyut-6. Isparitel braze coating (USSR)

1983. Salyut-7. Isparitel M, deposition (USSR)

1984. Salyut-7. UHT (USSR)

FIRST MANUAL OPEN SPACE WELD

1988. Mir, Yantar EB melt/weld (USSR)

1993. Parabolic CO_2 LBW (CAN)

1999. ISWE components went to MIR USA/UKRAINE/RUSSIA **CANCELLED**

Progress in Space Stagnated and Moved to Parabolic Flights

It has been over 50 years since NASA has performed a weld in space.

2021. SUBSA-BRAINS braze metal.

2023. Lockheed NASA Public-private JOINS.

2024. EBW in orbit by ThinkOrbital

2024. Parabolic fiber LBW Flight. Ohio State and NASA

Parabolic Vulkan experiment (USSR). 1965

Parabolic Skylab Materials (USA). 1972

Parabolic Nd:YAG LBW (USA). 1988/89

Parabolic UHT Experiment 1993

Parabolic ISWE Experiment 1994

Drop Tower GTA Weld Experiment 1998

Parabolic GHTA Weld Experiment 2001

2018. New Ukrainian EBW Gun Patented

2024. Early Stage Innovations grant

2024-2026. Early Career Initiative: LBW within TVAC

n.b.
Electron beam welding = EBW,
Laser beam welding = LBW

Why laser beam welding in space?

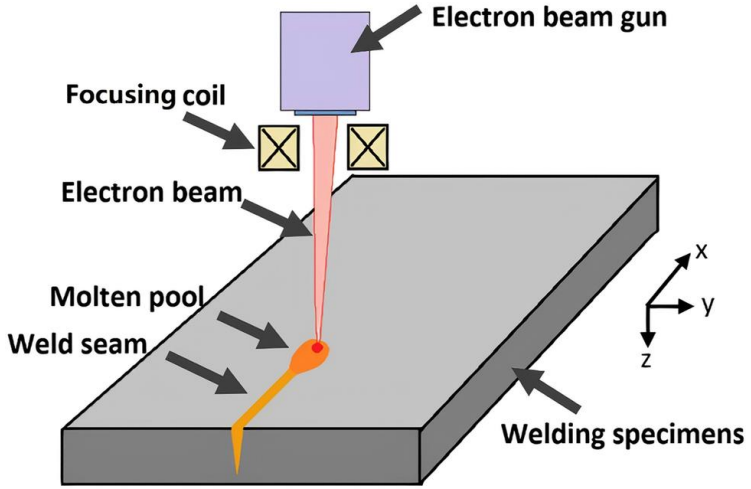

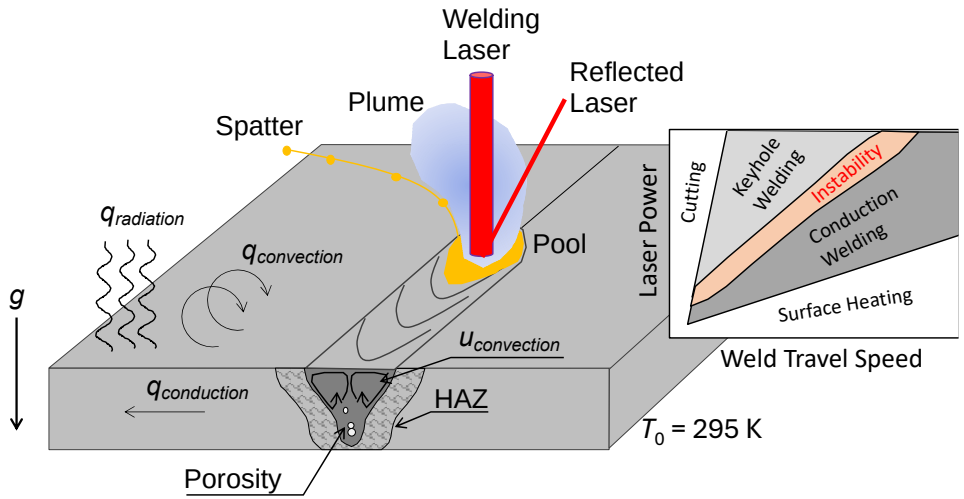

High-energy Beam Process → ↓ Criteria	Electron	Laser	Status
IVA flexibility (*e.g.* in habitat) & EVA flexibility (*e.g.* in vacuum, Lunar surface, on Mars)	●	○	Capability available after planned development
Workpiece variety (*e.g.* geometry, material)	◒	○	
Suitable for operation on end effector of robotic arm (*e.g.* EMI, mass, power delivery, heat rejection)	●	○	
Compatible with inspection tools & able to repair welds	●	○	
Power requirements & energy efficiency	○	◒	Commercial lasers
Suitable for additive manufacturing	◒	○	Future work (GCD, etc.)
Perform subtractive manufacturing – cutting, drilling, etc.	◒	○	
Capable of bending/forming structures	◒	○	
● - Poor ◒ - Satisfactory ○ - Good			

List adapted in part from: Tamir et al., *Thirtieth Space Congress*, 1993.

In-space conditions that influence welding

Variable	Case 1: In Space	Case 2: Chamber Inside Habitat	Case 3: Inside Habitat	Case 4: Lunar Surface	Case 5: Martian Surface	Baseline: Earth	Capabilities Needed at Present
Gravity	μg	μg	μg	0.17 *g*	0.38 *g*	1 *g*	μg to 0.38 *g*
Atmosphere	Vacuum (10^{-19} Pa)	Vacuum (10^{-4} Pa)	>21% O_2, <101 kPa	Vacuum (10^{-9} Pa) or habitat	95CO_2-2.6N_2-1.9Ar-0.2O_2-0.06CO (0.6 kPa) or habitat	78N_2-21O_2-0.9Ar-0.1other, 101 kPa	HV (10^{-1} Pa) UHV (10^{-5} Pa) XUHV (10^{-9} Pa)
Temperature	Extremely low ISS Exterior: 120 K – 395 K	~ 293 K	~ 293 K	40 K – 396 K	133 K – 300 K	~ 293 K	40 K – 400 K
Space Suit	Yes	No	No	Yes	Yes	No	

Table adapted and expanded from original source: Masubuchi, 1990, doi: 10.2207/qjjws1943.59.421

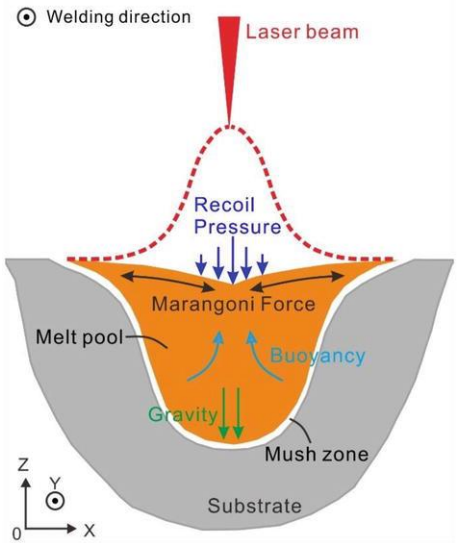

Licensed under CC BY 3.0 from Xiao *et al.*, 2021, doi: 10.5772/intechopen.97205

Reduced gravity is unique among the above effects in that it cannot be reproduced for prolonged periods on earth.

Current Work: Integrate existing capabilities across academia, government, and industry to investigate space environmental effects on welding processes to inform computational models, and to create public-private partnerships to develop and implement space welding technologies.

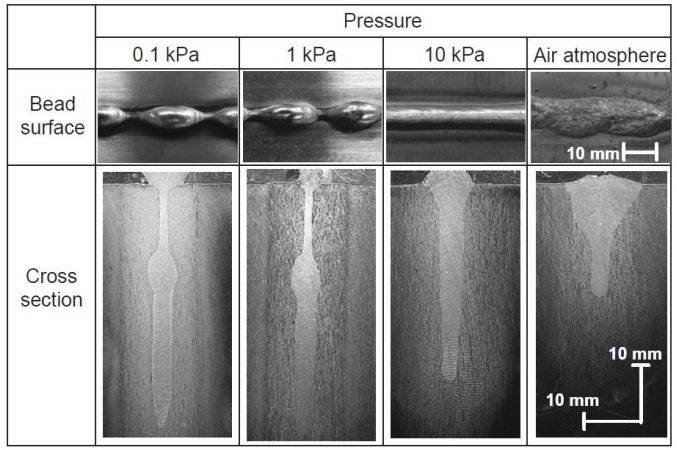

Licensed under CC BY-NC-ND 3.0 from Katayama et al., 2011, doi: 10.1016/j.phpro.2011.03.010.

Adapted in part from: Sowards, *American Welding Society Professional Program,* 2023.

Simulating space conditions for welding

Experimental platform → ↓ Criteria	Drop tower	Parabolic flight	Suborbital flight
Length of microgravity [s]	<5	20-25	>180
Gravity (quality) [g]	10^{-5}	10^{-3}-10^{-2} (up to 2.0)	10^{-4}
Mass allowed [kg]	10^{2}	10^{2}	10^{1}
Cost [$]	$	$$	$$$

Vacuum and Reduced Temperature

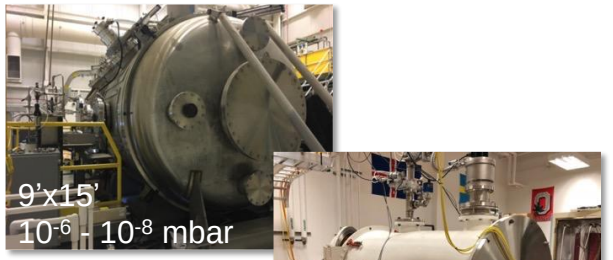

Example of MSFC capabilities to simulate reduced pressure / vacuum at 100 to 1000 km altitude.

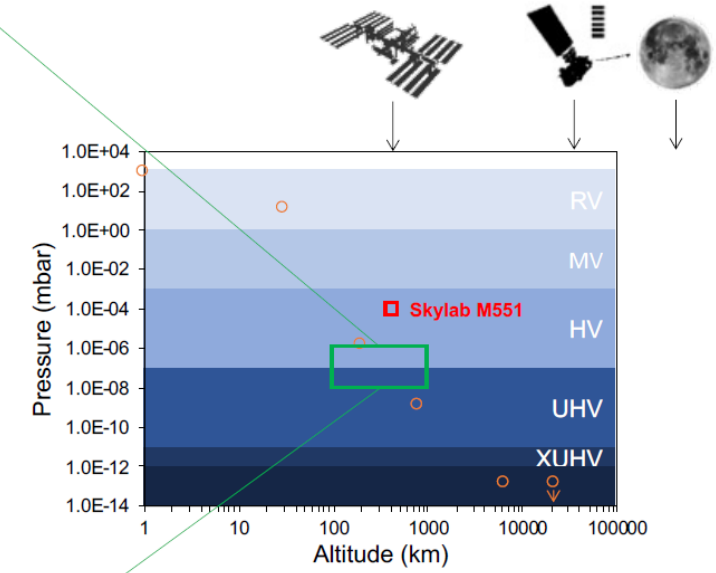

Microgravity / Reduced Gravity

Drop tower

Parabolic flight

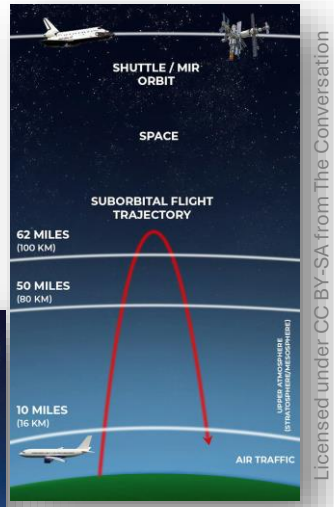

Suborbital flight

Low Earth Orbit (LEO)

μg

Lunar surface

0.17 *g*

Martian surface

0.38 *g*

Numerous experiments with welding systems in vacuum chambers on parabolic flights.

Mladenov, Koleva, and Trushnikov, *E+E*, 2019.

Adapted in part from: Sowards, *American Welding Society Professional Program,* 2023.

Key effects to consider for in-space LBW

Red boxes indicate instrumentation and modeling opportunities.

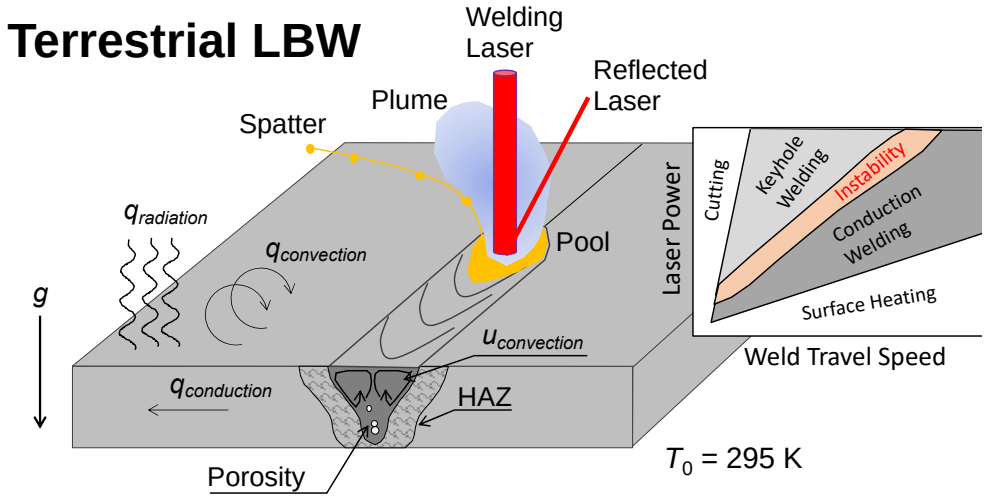

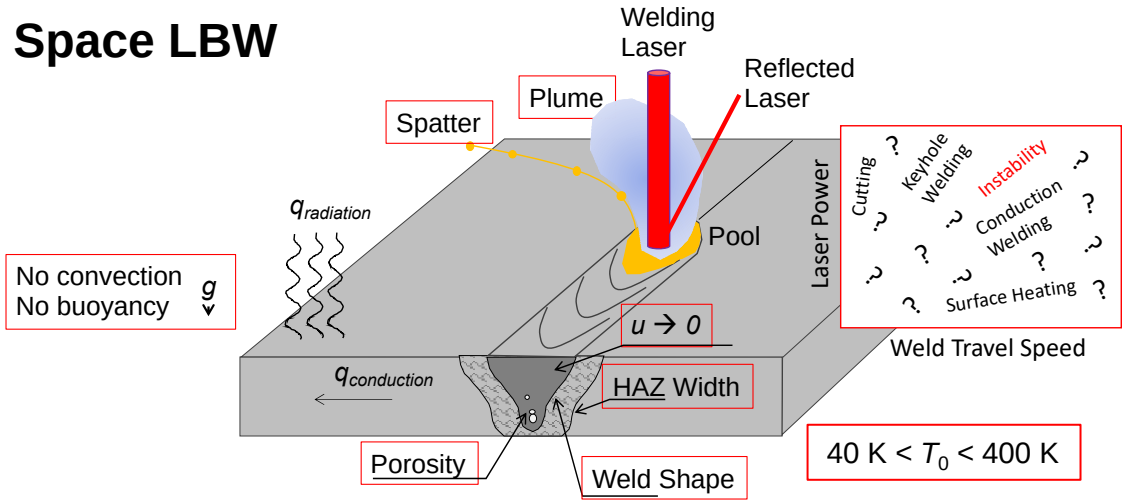

Issue #1 Weld heat transport has profound effect on size of a weld (especially fusion zone, FZ, and heat affected zone, HAZ) and its metallurgical transformations and hence weld properties:

Temperature gradient and cooling rate are proportional to thermal conductivity and T_0^2

Issue #2 Reduced gravity reduces buoyancy-induced convection:

Development of weld pool shape and porosity evolution are altered, and chemical effects become dominant, e.g., surface-active elements influence weld penetration due to thermocapillary flow. (minute alloy chemistry changes are important)

Issue #3 Reduced pressure/vacuum in space:

Heat transport is dominated by radiation and conduction rather than by convection. Weld shape and width, and weld strength will be influenced by change in weld cooling.

Reduced pressure influences laser beam keyhole stability, evaporation of volatile species, safety issues, etc.

From: Sowards, *American Welding Society Professional Program*, 2023.

Progression of flight experiments

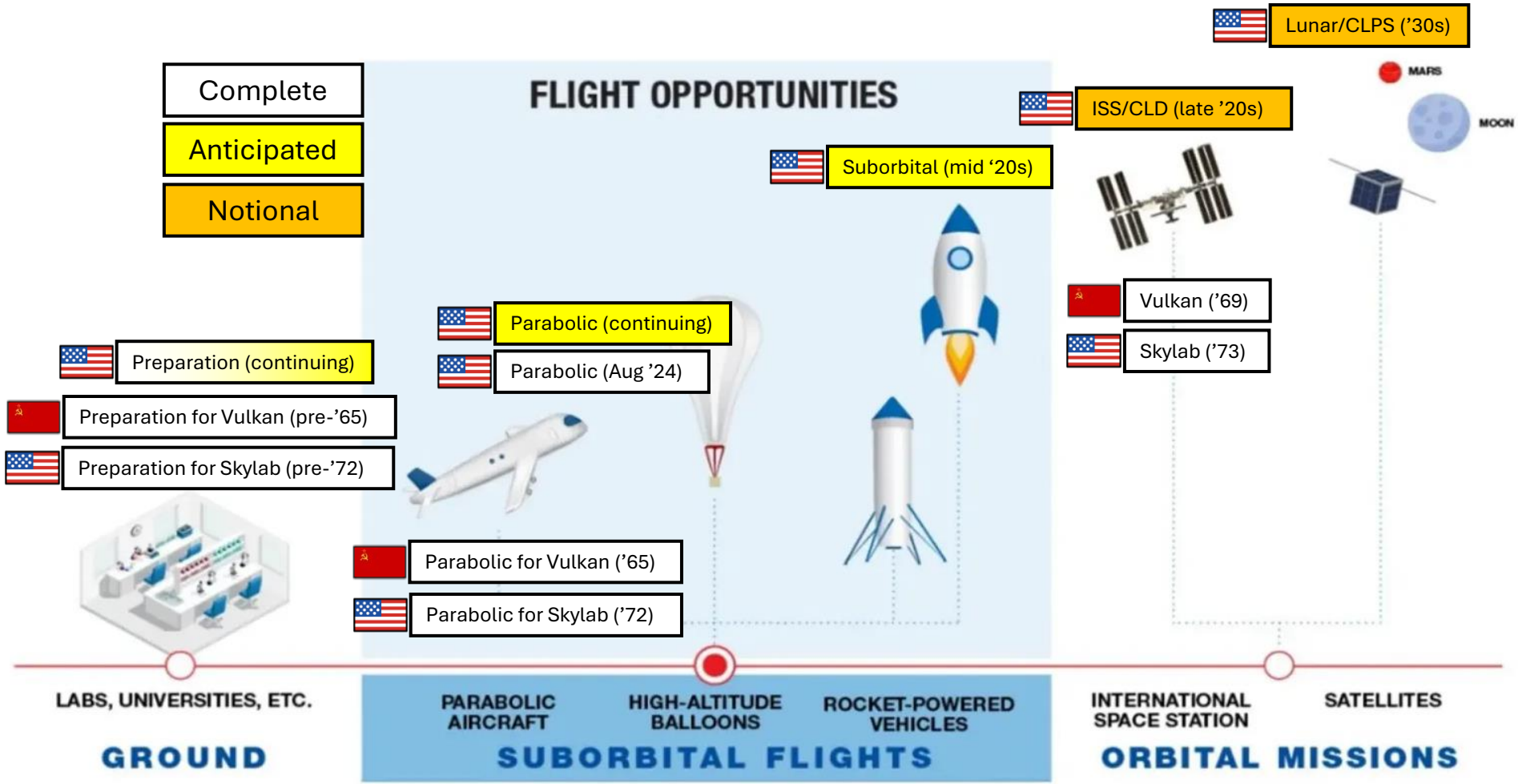

Concurrent development of Digital Twin using collected data

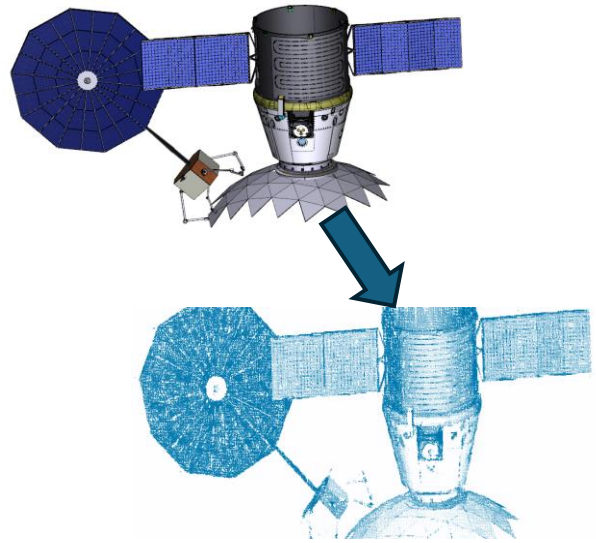

Underlying graphic from Kelly *et al.* in *ASCEND 2020*, 2020. doi: 10.2514/6.2020-4135. USG work.

Progression of flight experiments

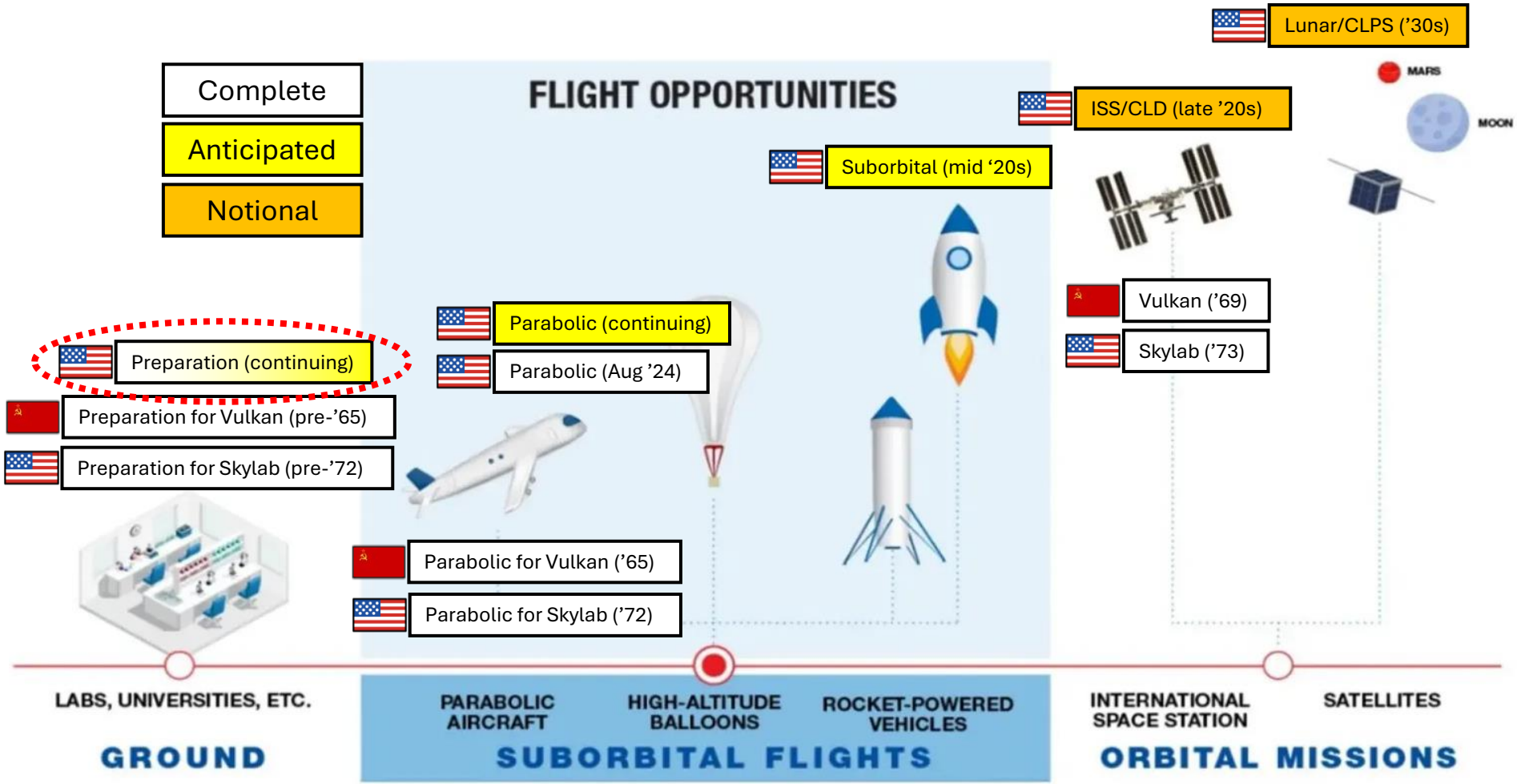

Concurrent development of Digital Twin using collected data

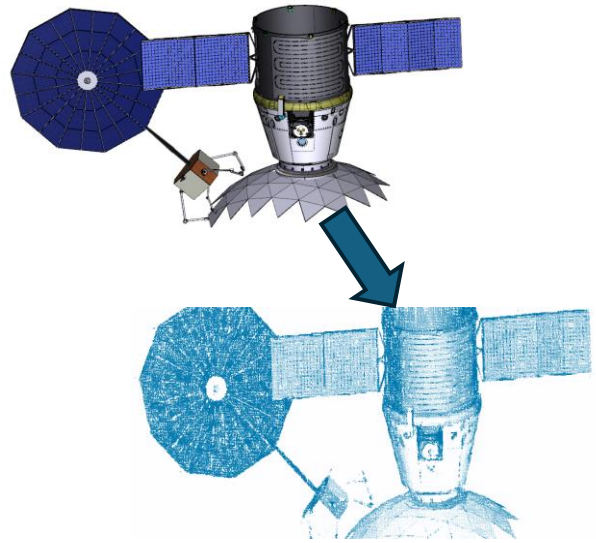

Underlying graphic from Kelly *et al.* in *ASCEND 2020*, 2020. doi: 10.2514/6.2020-4135. USG work.

Ground testing LBW on 3-DOF "Flat Floor"

Enclosed LBW station for rapid parameter development

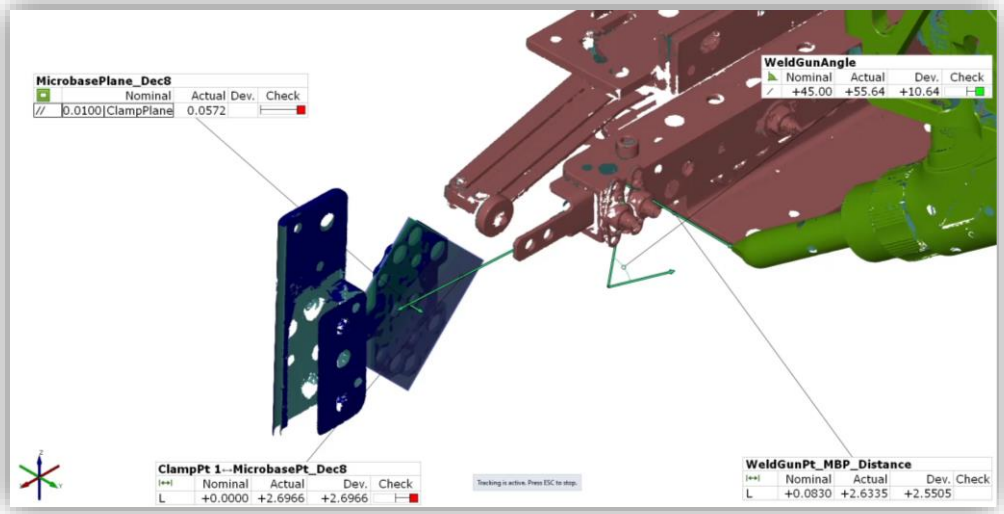

Structured light scan of joint fit-up on Flat Floor

Half of joint on mobile base, other half on floating robotic arm; LBW from side; *in situ* videography and thermography

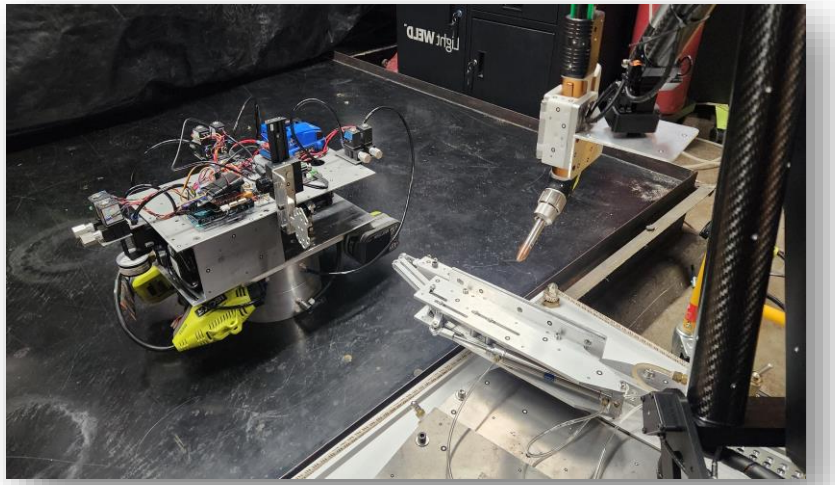

Ongoing:
Glovebox capable of variable composition atmosphere and with regolith simulant (Lunar, Martian, etc.) via handheld LBW

Progression of flight experiments

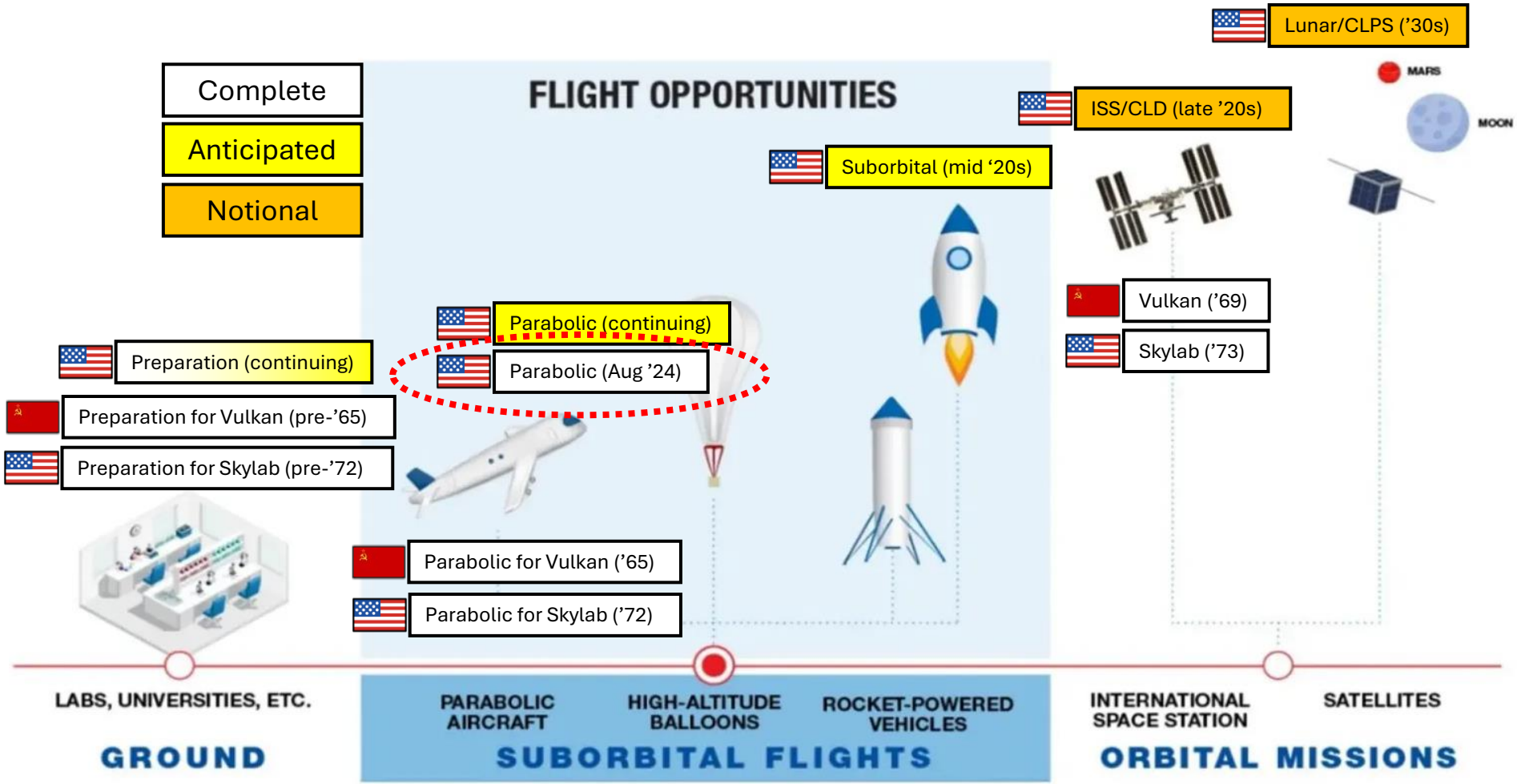

Concurrent development of Digital Twin using collected data

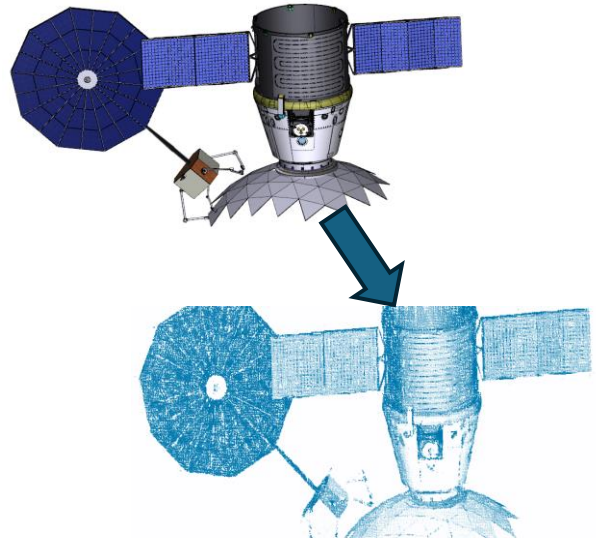

Underlying graphic from Kelly *et al.* in *ASCEND 2020*, 2020. doi: 10.2514/6.2020-4135. USG work.

Collaboration with Ohio State University on parabolic LBW

Integration and Ground Demonstration of Self-contained Laser Welding System for Parabolic Microgravity Experiments.

- OSU. Profs: Ramirez, Panton, Horack, Nassiri, Williams, Nate Ames, Bob Rhoads. Undergrad capstone team. Grad students: Eugene Choi, Aaron Brimmer, Will McAuley.
- NASA. Jeff Sowards, Karen Taminger (LaRC), Will Evans, Zach Courtright, Louise Littles, Andrew O'Connor, Emma Jaynes, Ben Rupp, Tom Bryan.

Heritage parabolic vacuum chamber from NASA/LaRC

Laser Beam Welding

Courtesy: IPG Photonics

Modern high-power fiber lasers enable LBW for space; Welding times within microgravity parabola length (15-20 seconds)

Generate Model Calibration Data

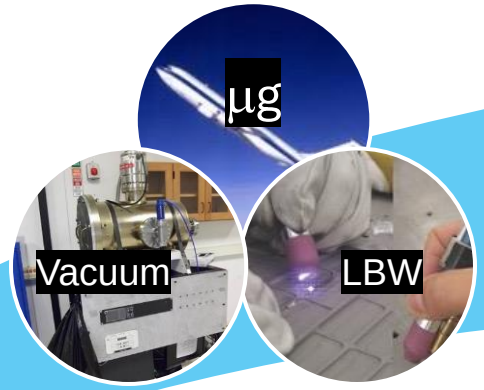

OSU-NASA CAN

Leverage LBW expertise and workforce development at OSU

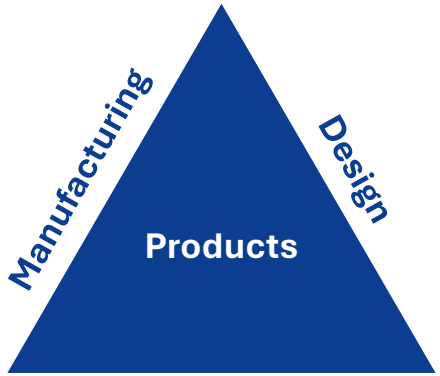

Integrated Computational Materials Engineering (ICME)

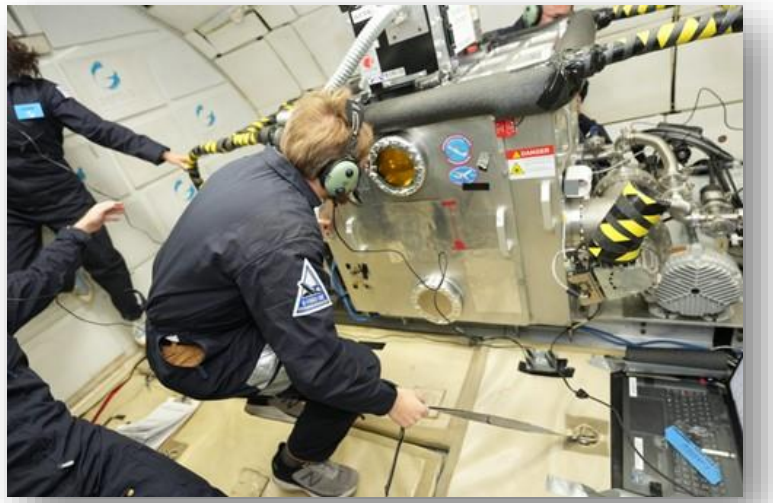

Retrofitted vacuum chamber in flight on Zero-G 727 aircraft

Adapted in part from: Choi, *Worldwide Advanced Manufacturing Symposium* (2024).

Progression of flight experiments

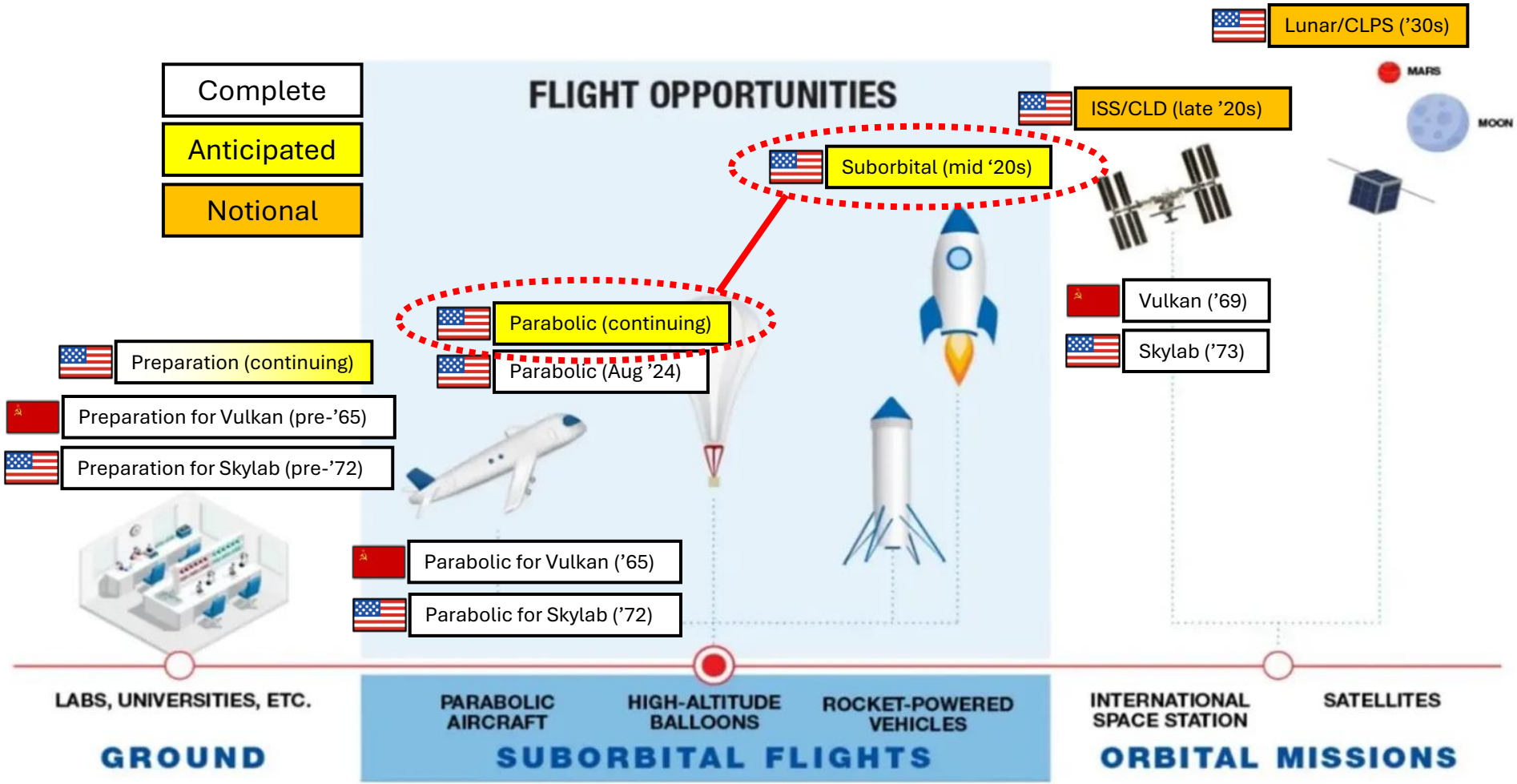

Concurrent development of Digital Twin using collected data

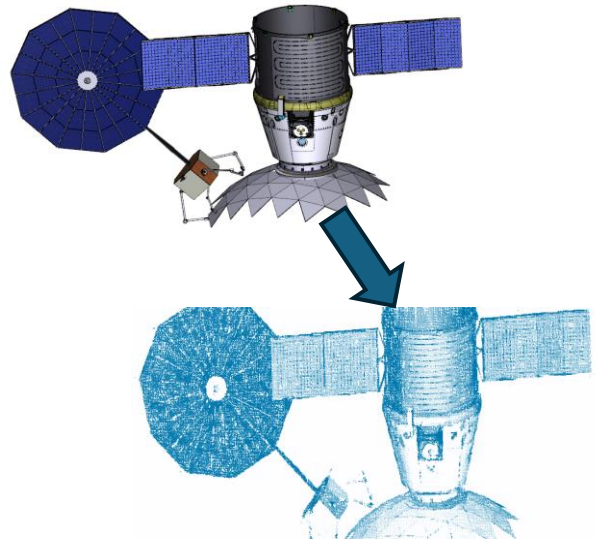

Underlying graphic from Kelly *et al.* in *ASCEND 2020*, 2020. doi: 10.2514/6.2020-4135. USG work.

Evolve from parabolic to suborbital flight experiments

Parabolic	Suborbital
Tens of seconds in reduced or μg	Minutes in reduced or μg
Two-*g* during pull out (weld solidified?)	Hi-*g* only before welding (launch)
g-jitter complicates effect of gravity	Reduced *g*-jitter

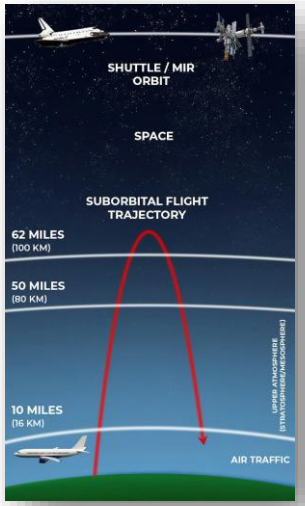

Initial protoflight hardware design

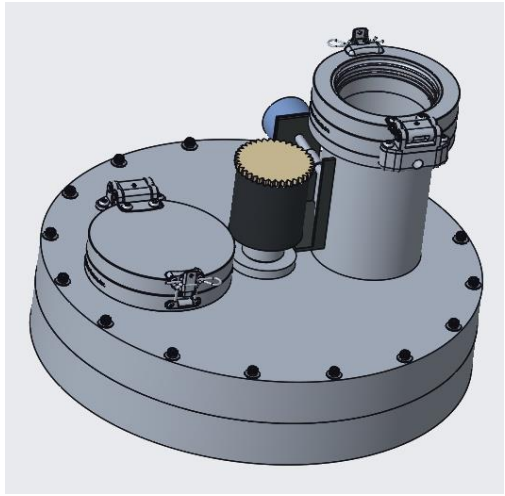

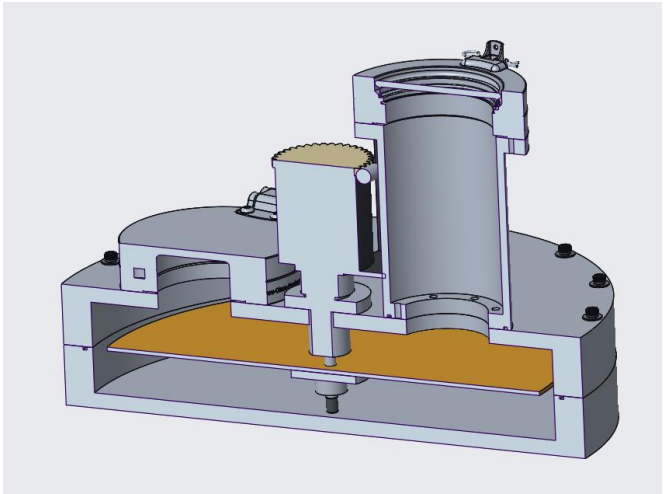

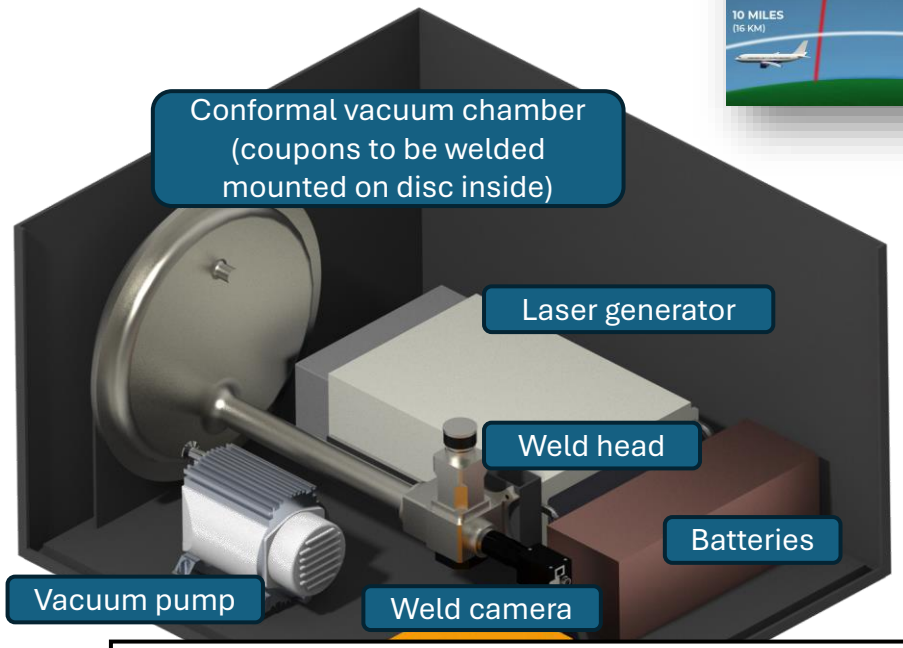

Conceptual design developed with MSFC Advanced Concepts Office

Thermal and structural modeling

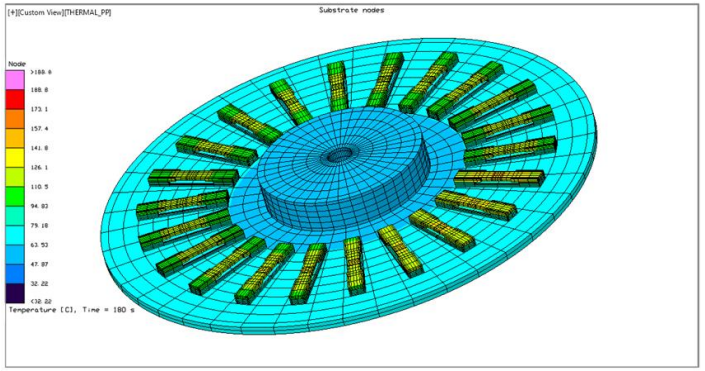

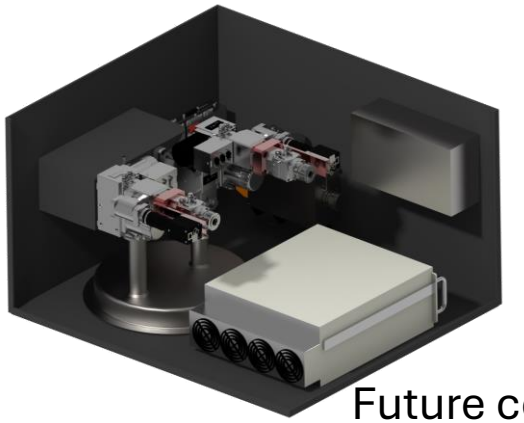

Future concept: multiple weld heads

Practicalities of suborbital LBW

Laser module selected: 1500 W peak pulsed power, 1070 nm, Yb fiber

Requires batteries (excessive power draw from flight platform)

Fully automated control

Investigating (via ground testing) concerns re:

- Vapor deposition and spatter on vacuum window
- Loss of vacuum due to off-gassing

Courtesy: IPG Photonics

Materials selected: stainless steel 316L, aluminum 2219-T87, Ti64

Also considering Al-Cu binaries:

- More tractable for computational models
- Previous flight experiments investigated solidification (Al-4wt%Cu in 1*g* and *ug* shown below)

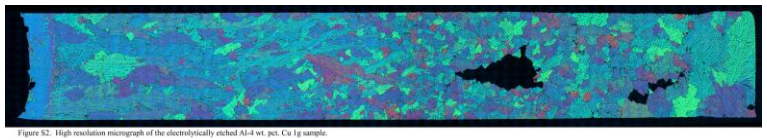

Figure S2. High resolution micrograph of the electrolytically etched Al-4 wt. pct. Cu 1g sample.

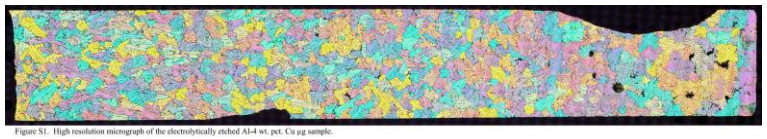

Figure S1. High resolution micrograph of the electrolytically etched Al-4 wt. pct. Cu μg sample.

Beckermann, C, "Solidification Using a Baffle in Sealed Ampoules Effect of Convection on the Columnar-to-Equiaxed Transition in Alloy Solidification" NASA Physical Sciences Informatics (PSI). https://psi.ndc.nasa.gov/app/record/204999

Data collection to anchor computational models

- Weld camera: 140+ dB HDR imaging for weld bead size & morphology
  - Coxial mount onto weld head for on-line alignment with specimens
- Thermal/weld camera: SWIR (InGaAs) thermography of weld
  - Reduced effect of emissivity shifts on thermal data
  - Enhanced view through weld fumes
- Thermocouples: provide calibration for thermography
  - Establish workpiece starting temperature (collateral heating)
  - Require slip ring (or similar) and pass-through into vacuum
- Plume characterization (ground only)
  - Spectrometer for chemistry; mid-wavelength IR or Schlieren for morphology

Latest prototype status – design and fabrication

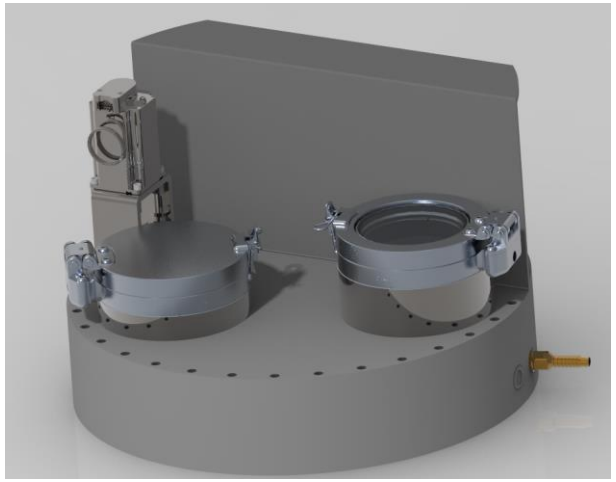

- Switched from central spindle to turntable driven by ring gear
- Added additional access door
- Reduced length of “stovepipe”
- Provided mounting plane for weld head, etc.

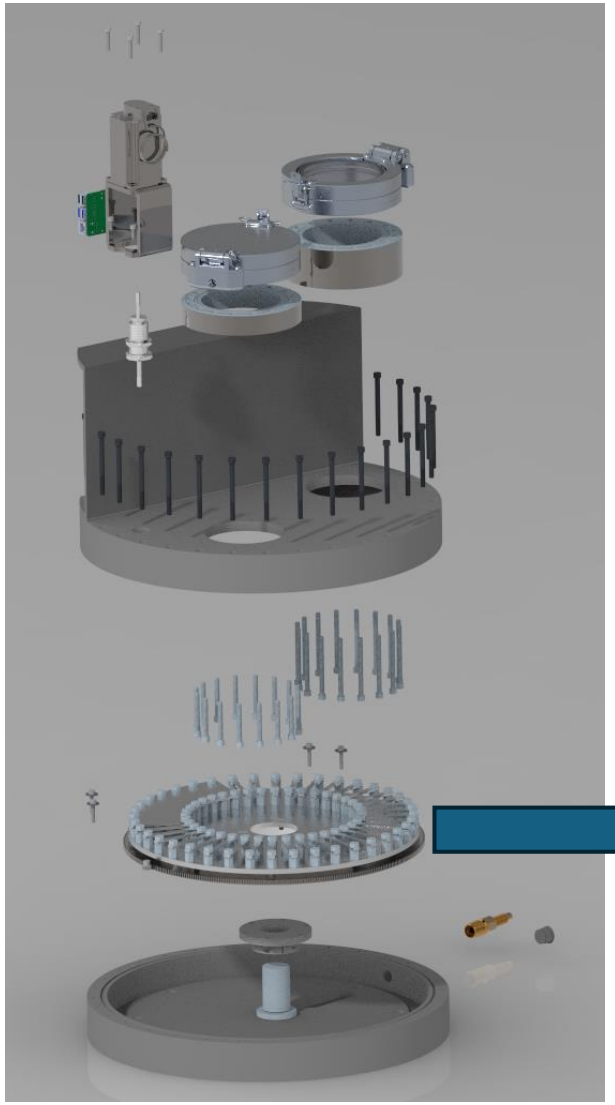

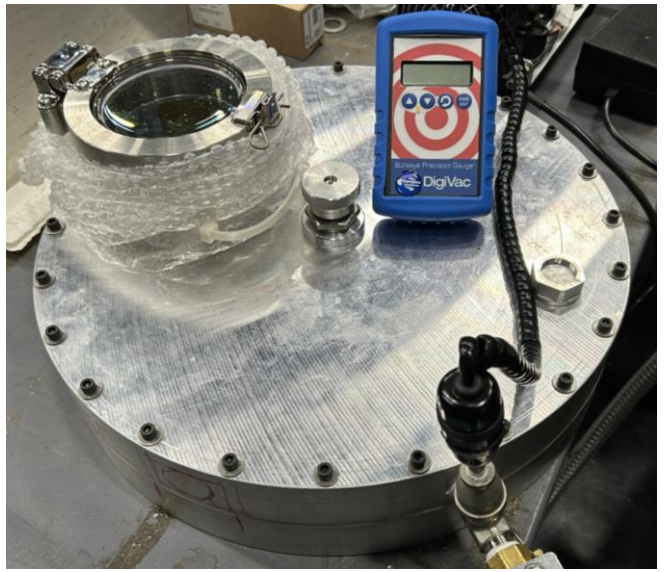

- Vacuum chamber robust and maintains <100 Pa
- Initial operating capability (spot welds without thermography) expected shortly

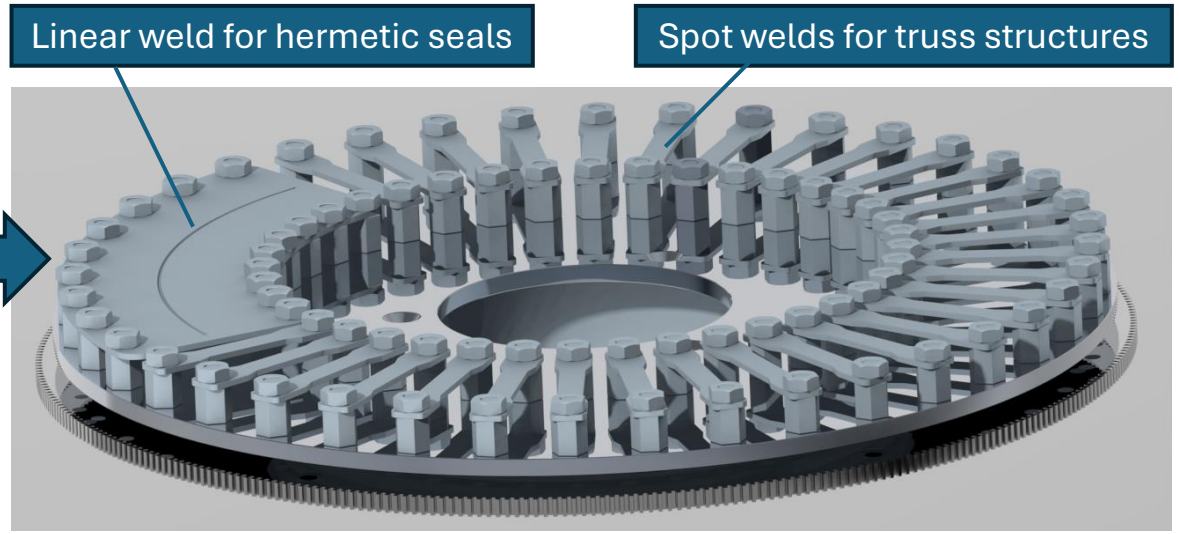

Latest prototype status – initial operating capability

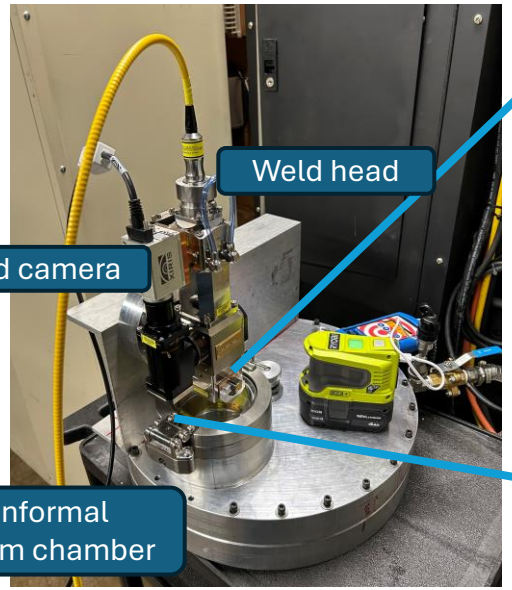

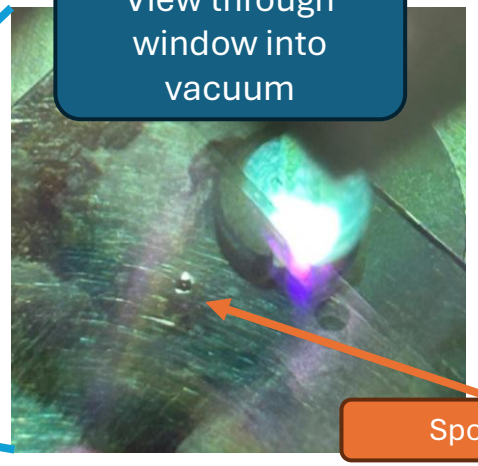

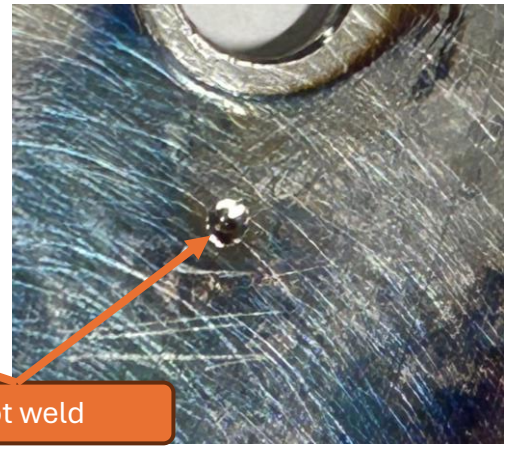

Coaxial weld camera in operation; thermal to follow

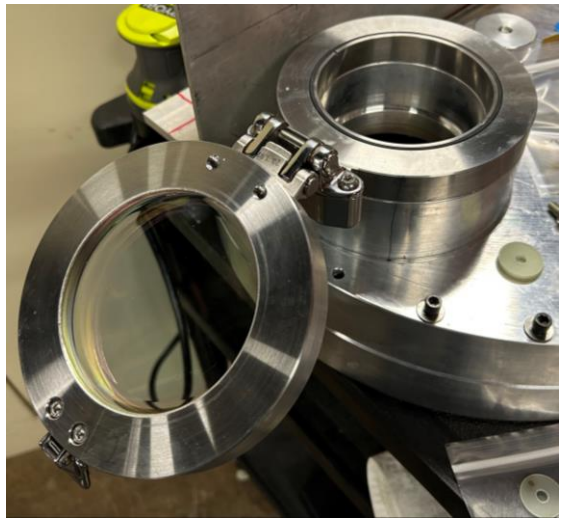

Rapid access to coupons

Concern: metal vapor coating, also spatter
Current mitigation: sacrificial glass
Investigating other mitigations

Progression of flight experiments

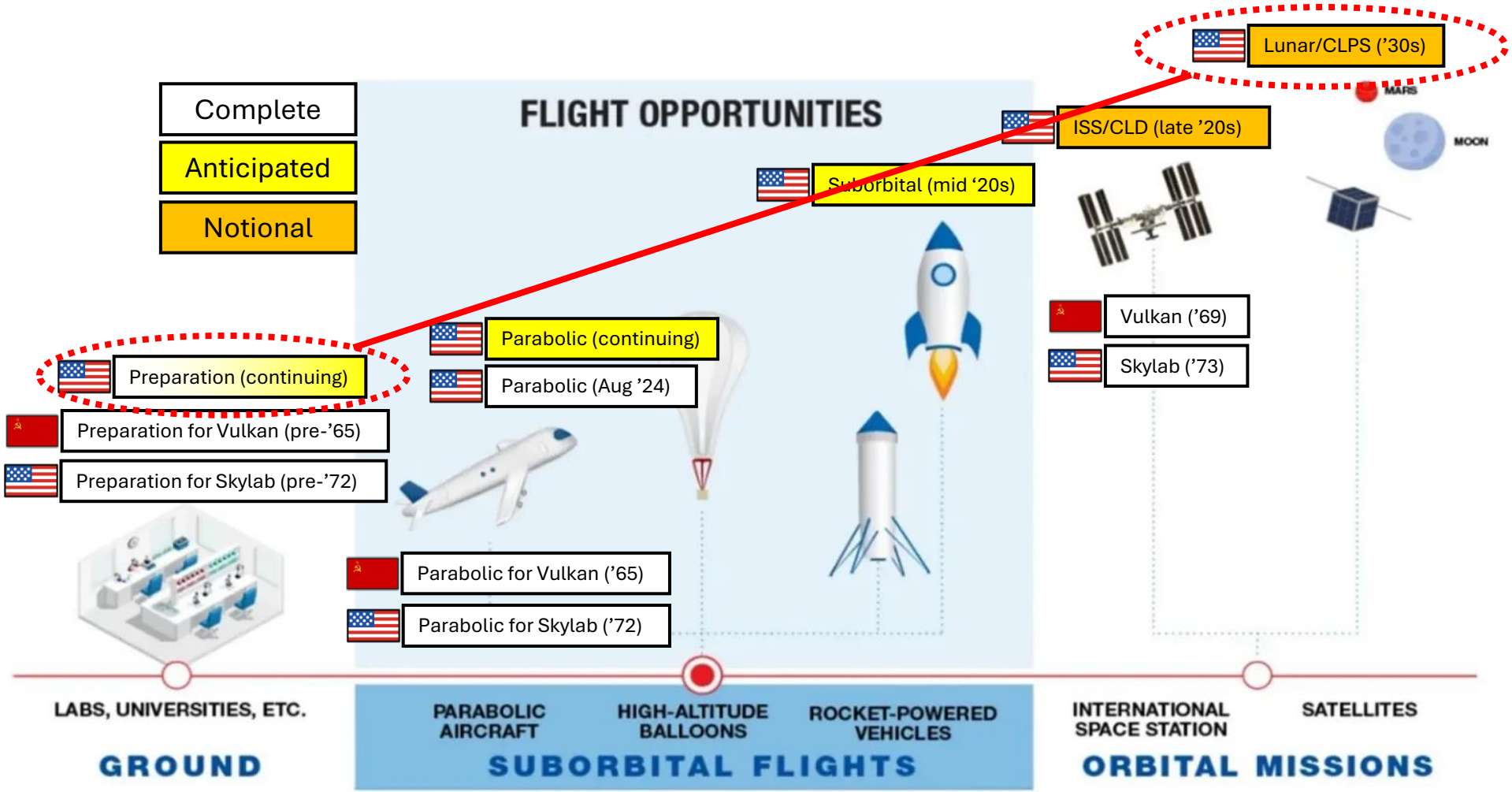

Concurrent development of Digital Twin using collected data

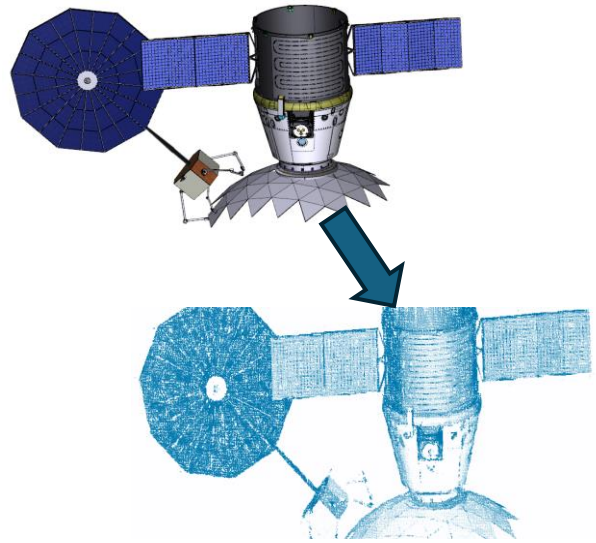

Underlying graphic from Kelly *et al.* in *ASCEND 2020*, 2020. doi: 10.2514/6.2020-4135. USG work.

Lunar Assembly and Servicing by Autonomous Robotics (LASAR)

NASA-funded Early Career Initiative project: Mature LBW and associated robotics & NDE for Lunar infrastructure applications

- Ruggedized laser optics and robotic arm suitable for thermal vacuum
- Supervised autonomous LBW
- Non-contact NDE of welds

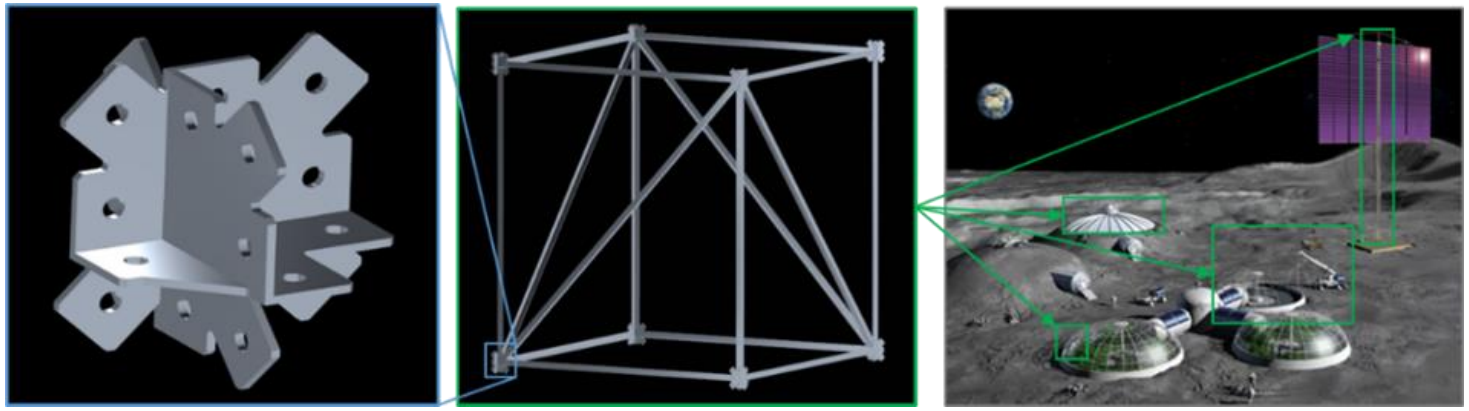

PI: Andrew O'Connor; PM: Zach Courtright (both MSFC)

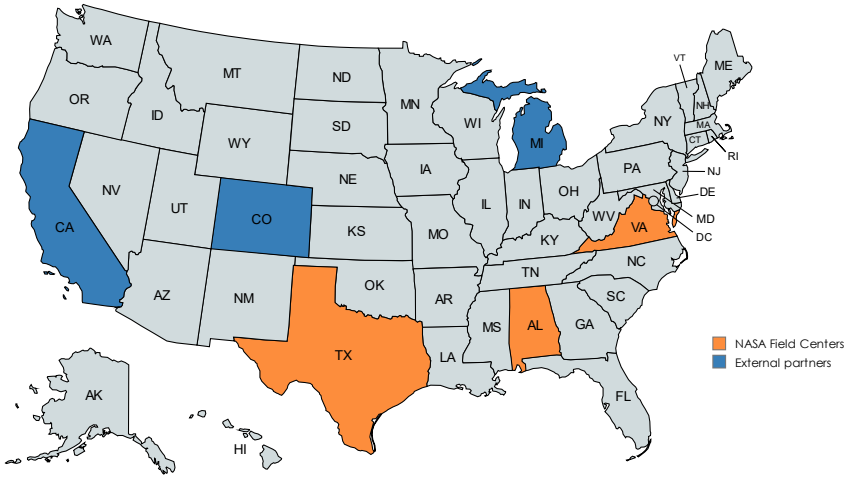

NASA Core Team Members

Name	Center
Emma Jaynes	NASA/MSFC
Alex Sowell	NASA/JSC
Raju Subedi	NASA/MSFC
Brace White	NASA/LaRC
Supported by:	
William Evans	NASA/MSFC
Matthew Mahlin	NASA/LaRC
Parker Shake	NASA/MSFC

External Partners

Name	Role
Laserline	Laser Processing Partner
Motiv Space Systems	Robotics Hardware Partner
PickNik Robotics	Robotics Software & Autonomy Partner

Mentors

Name	Role
Shaun Azimi	JSC Robotics SME
Bill Doggett, PhD	LaRC In-Space Assembly SME
John Fikes	MSFC Management SME
Jeffrey Sowards, PhD	MSFC Laser Welding SME

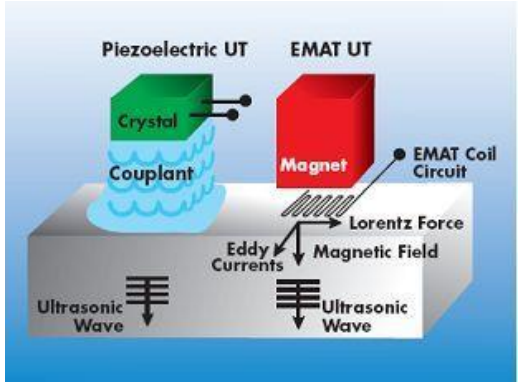

Electromagnetic acoustic transduction (EMAT) for NDE

Demonstration of hand-welded Snowflake joint

- Hand-welding gives insight on joint re-design to improve accessibility for welding, to indicate ideal weld placement, and to inform robotic welding

- Extensible to laser wire directed energy deposition (LW-DED); similar to wire-fed welding & weld repair

DARPA Novel Orbital and Moon Manufacturing, Materials, and Mass-efficient Design (NOM4D) – TVAC laser forming (LF)

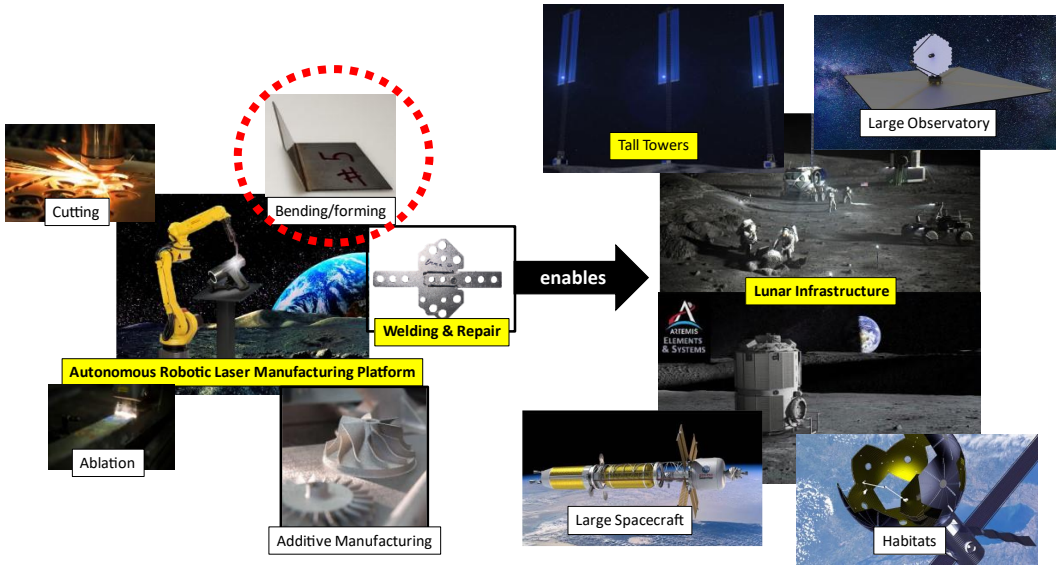

Image credit: ThinkOrbital, www.mechanicalcaveman.com

Credit: University of Florida

Form complex geometries with minimal pre/post-processing or workpiece setup

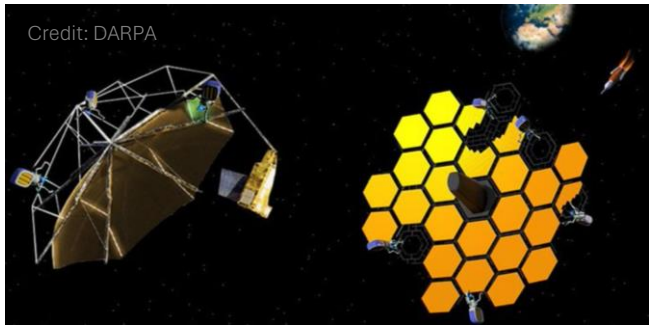

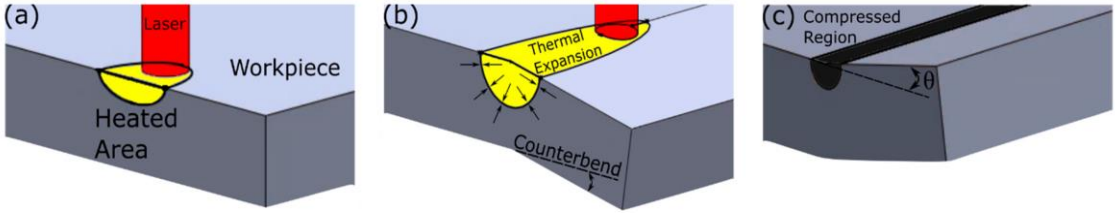

Thermal Gradient Mechanism (TGM) enables bending towards laser beam

- University of Florida (UF) demonstrating laser forming (bending of sheet metal) under vacuum
- MSFC extending laser bending to thermal vacuum (TVAC) environment
- Excellent synergy with ISW, especially LBW
- Employing Integrated Computational Materials Engineering (ICME) – thermal modeling, thermodynamics and precipitation, grain growth, etc. – to leverage thermal history of workpiece to predict microstructure and performance

Rapid advancement in state-of-art for LF under vacuum via multi-disciplinary team

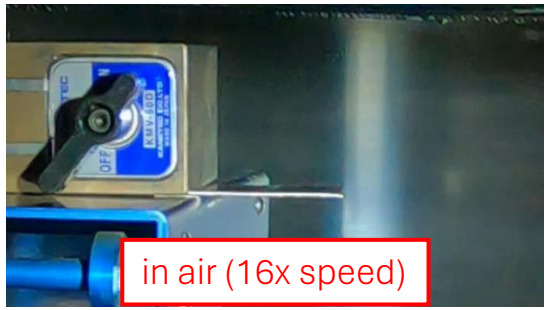

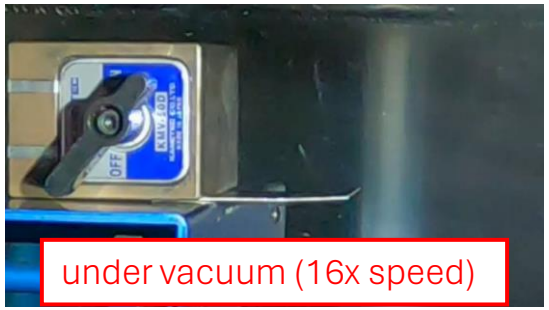

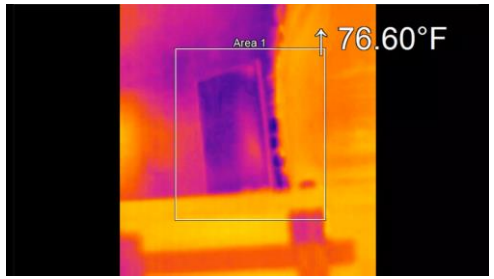

Long-wave infrared thermography

Less than two weeks from authority to proceed to initial demonstration of laser forming in air and under vacuum!

SOA advanced: Vacuum (~10^{-3} Pa/10^{-5} Torr) greater than achieved previously

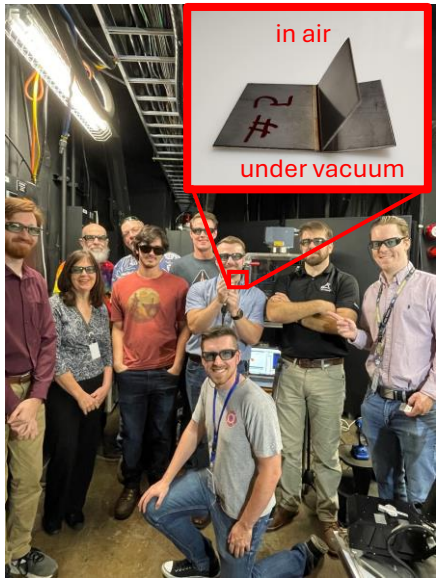

Initial laser bending demonstration team

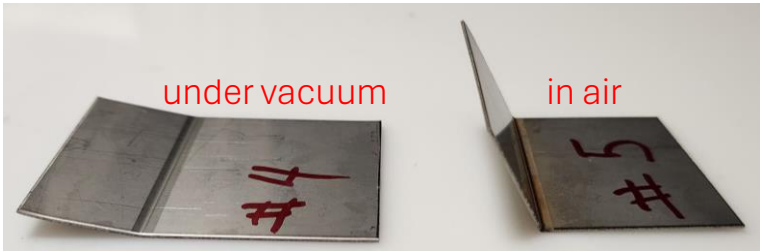

Laser bent AISI 304 stainless steel, 0.6 mm thick

Existing TVAC refitted to enable laser forming at cryogenic and elevated temperatures

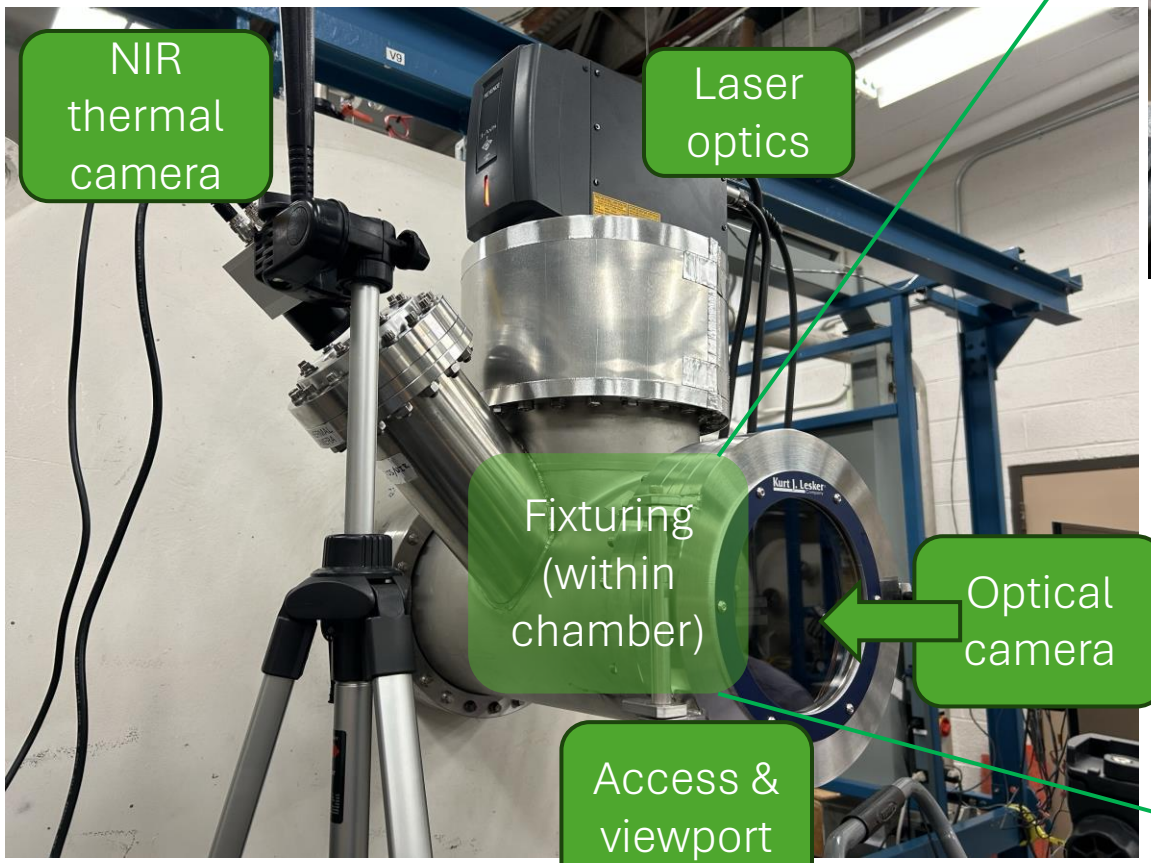

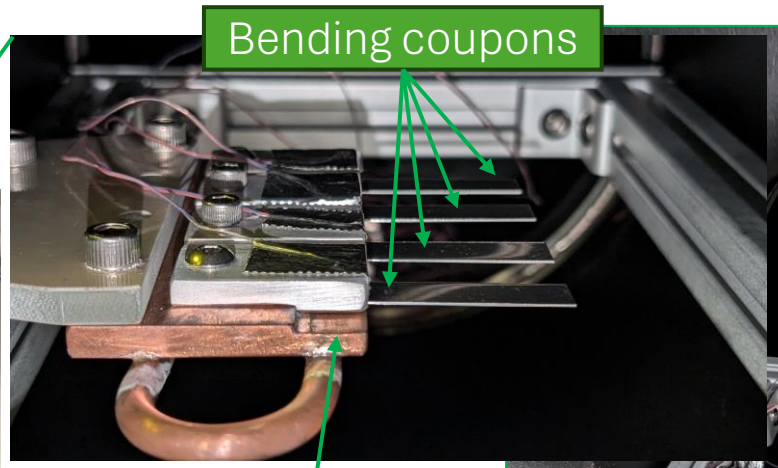

GN2 circulates for thermal conditioning of copper block

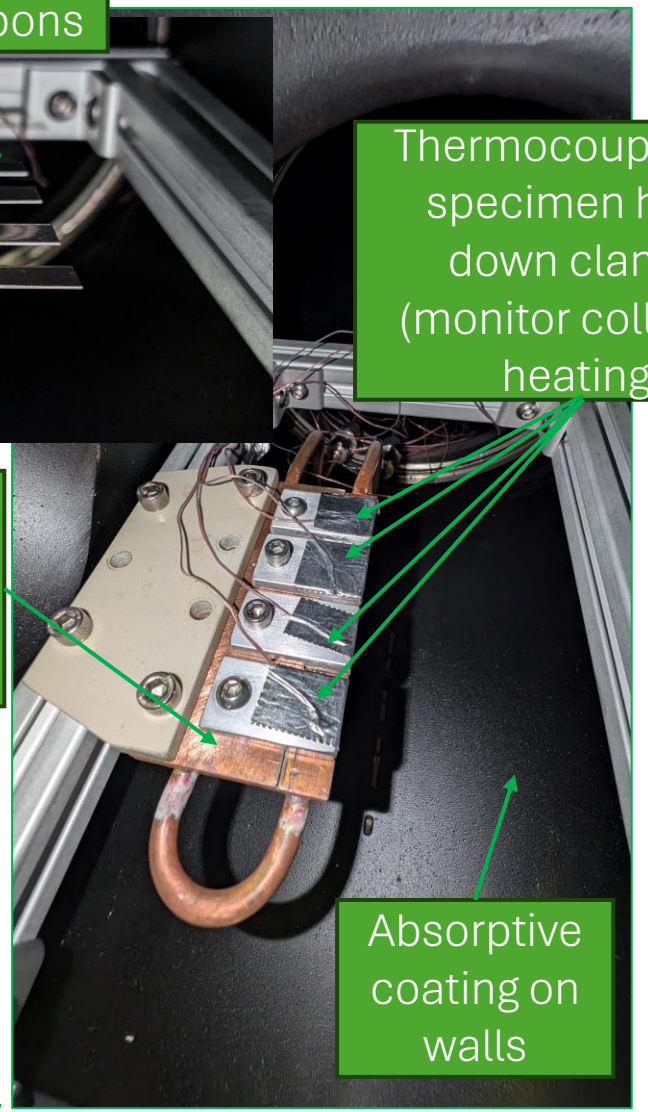

Remarkably consistent bending in TVAC at same linear energy density for 304SS

Linear fit model for 304SS gave confidence to proceed to TVAC trials

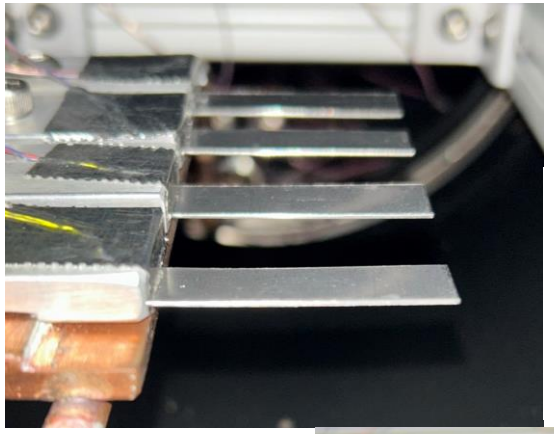

304SS strips bent at -120°C workpiece initial temperature under vacuum

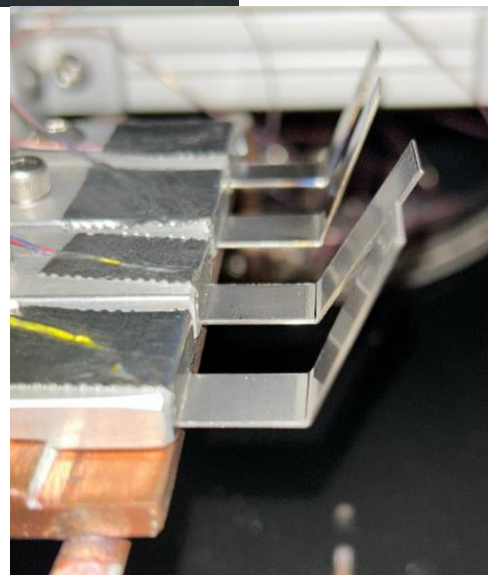

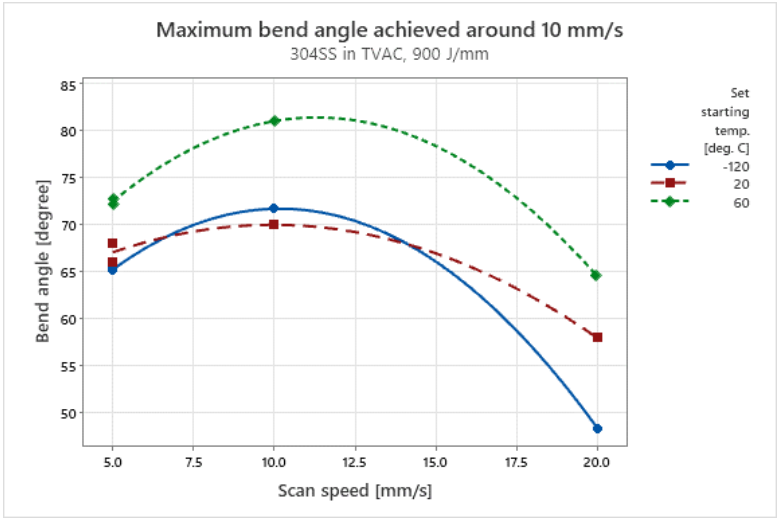

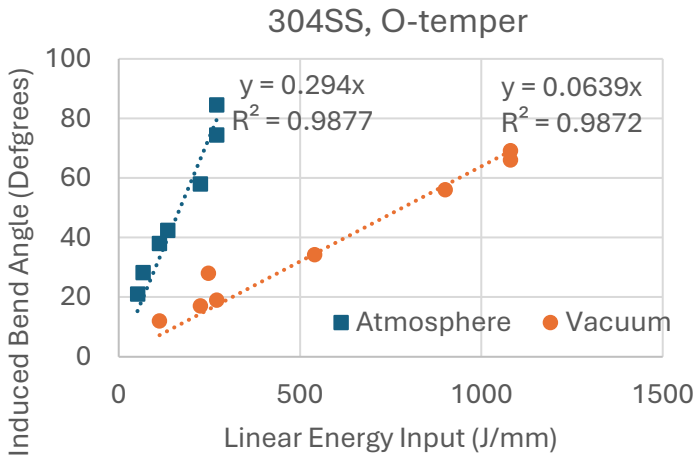

Relative insensitivity to process parameters points towards domination by thermophysical properties for 304 SS (low thermal diffusivity).

In operando monitoring of laser forming in TVAC

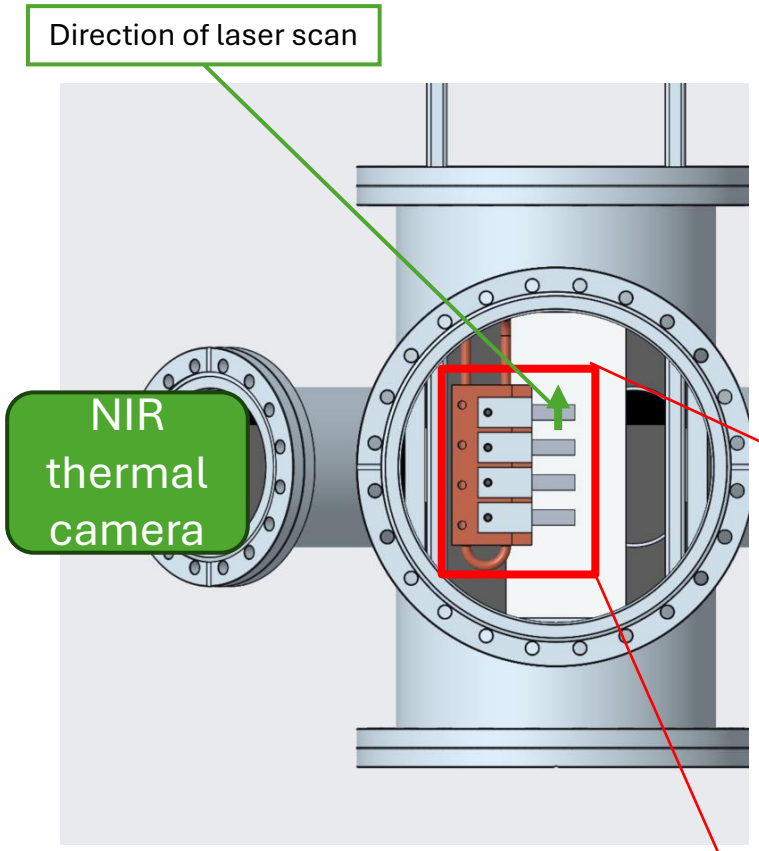

Top-down render of T-junction on TVAC, indicating bend region

n.b. IR thermography not calibrated, cannot give absolute values but suitable for trends analysis; 600°C is lower limit of NIR thermal camera (Optris PI 08M)

Thermograph of bend region

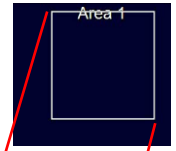

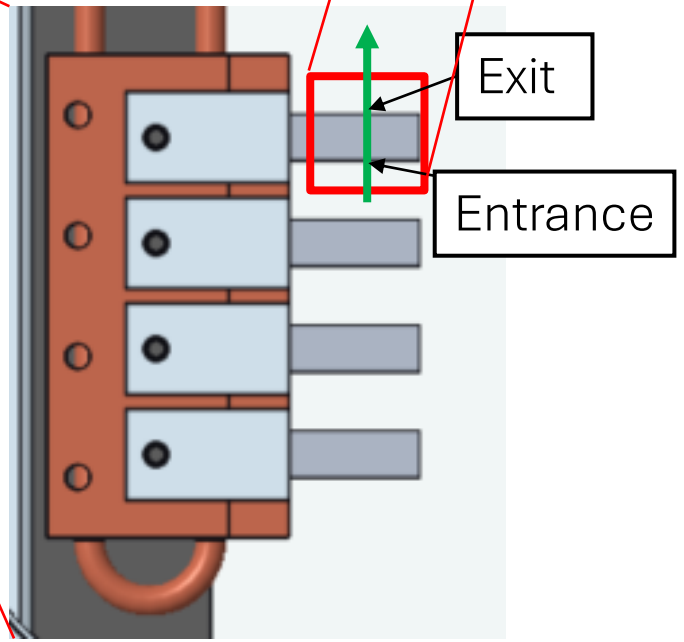

Edge-on view of bending with per-pass angle calculation (16x speed)

Correlating bend-per-pass measurements with thermography will reveal underlying mechanism and accelerate technology maturation.

Explanation of thermography data

- NIR thermal camera pointed at top surface of bend region
- Pass average: averaged over width of etched region
- Pass max: maximum temperature recorded during each frame of pass (beam spot)
- Entrance: temperature at entrance point
- Exit: temperature at exit point

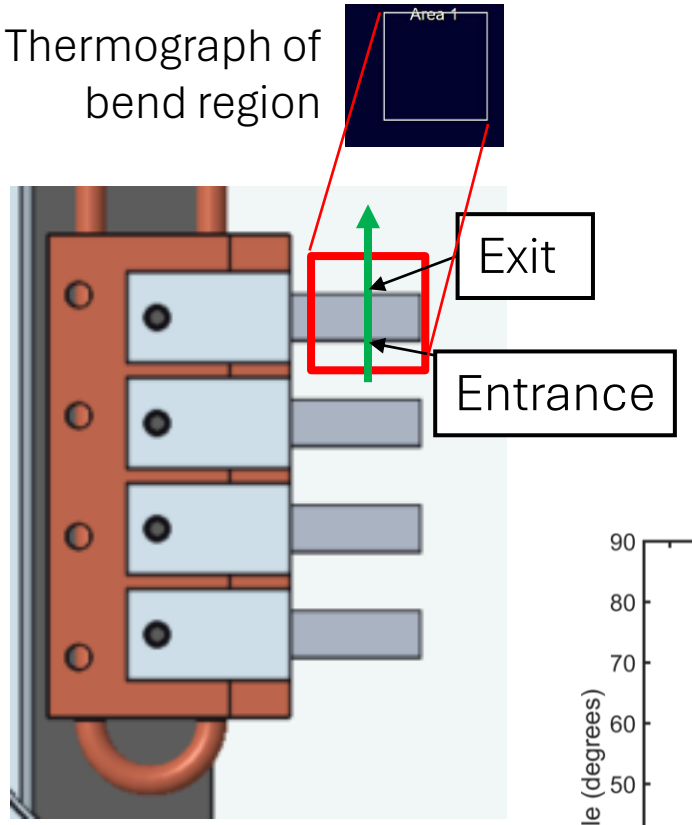

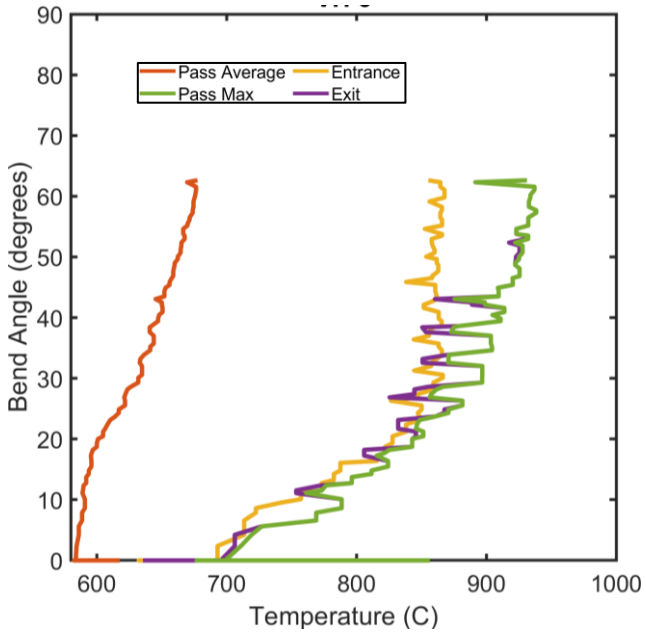

Scan speed and bend angle linked to thermography

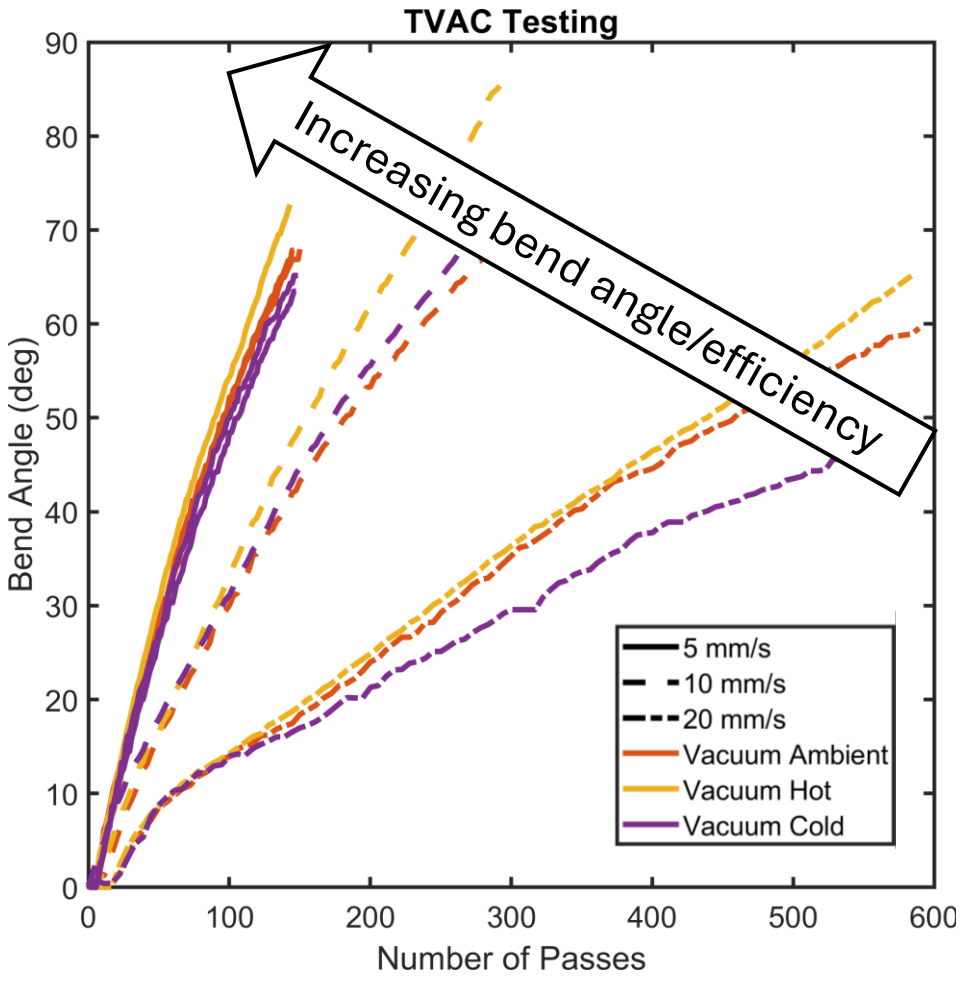

Strongly increasing bend angle with increasing scan speeds (at left) linked to faster temperature saturation from thermography (at right)

Longer time at saturation temperature leads to more bending (?)

Points towards domination by thermophysical properties for 304SS (low thermal diffusivity)

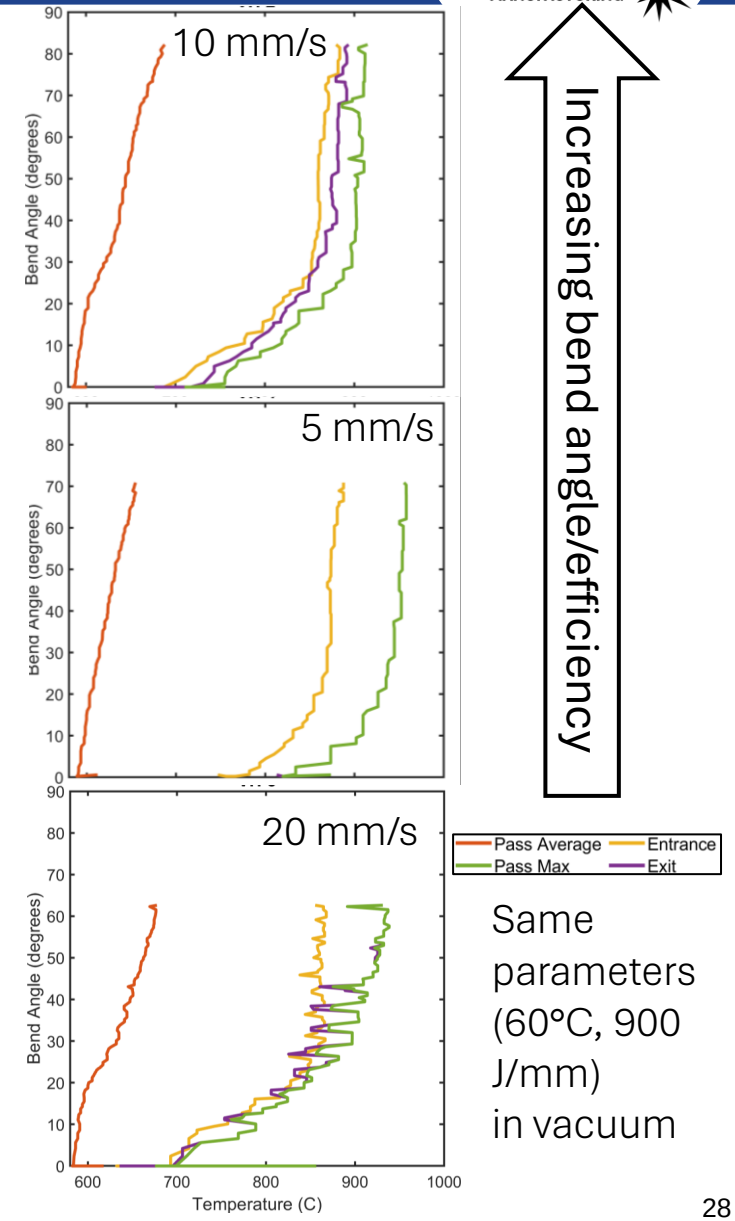

Same parameters (60°C, 900 J/mm) in vacuum

Workpiece initial temperature and bend angle linked to thermography

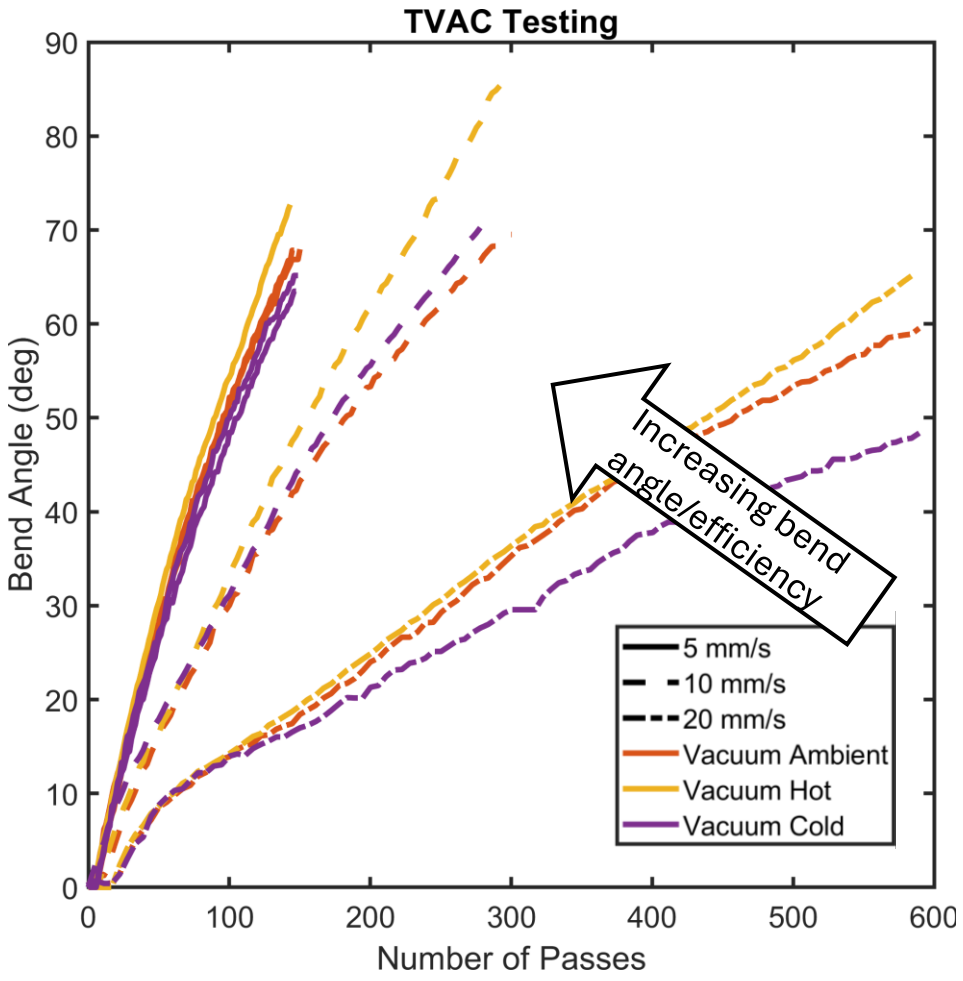

Weakly increasing bend angle with increasing workpiece initial temperature (at left) linked to lower saturation temperatures at colder starting temperatures from thermography (at right)

Lower saturation temperature leads to reduced bending (?)

Points towards domination by thermophysical properties for 304SS (low thermal diffusivity)

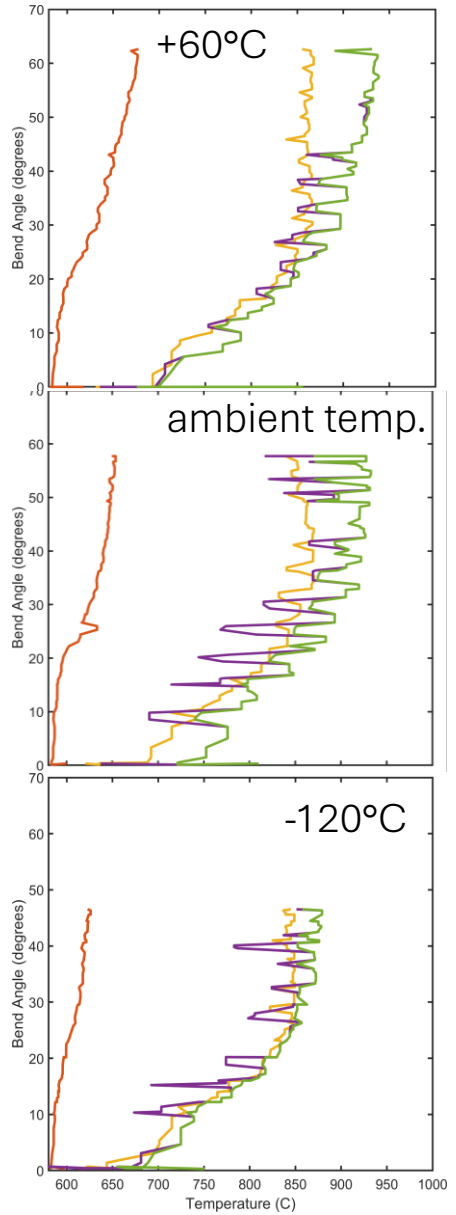

increasing bend angle/efficiency

Same laser parameters (20 mm/s, 900 J/mm) in vacuum

Structured light scans reveal distortion

Atmosphere, ambient temperature

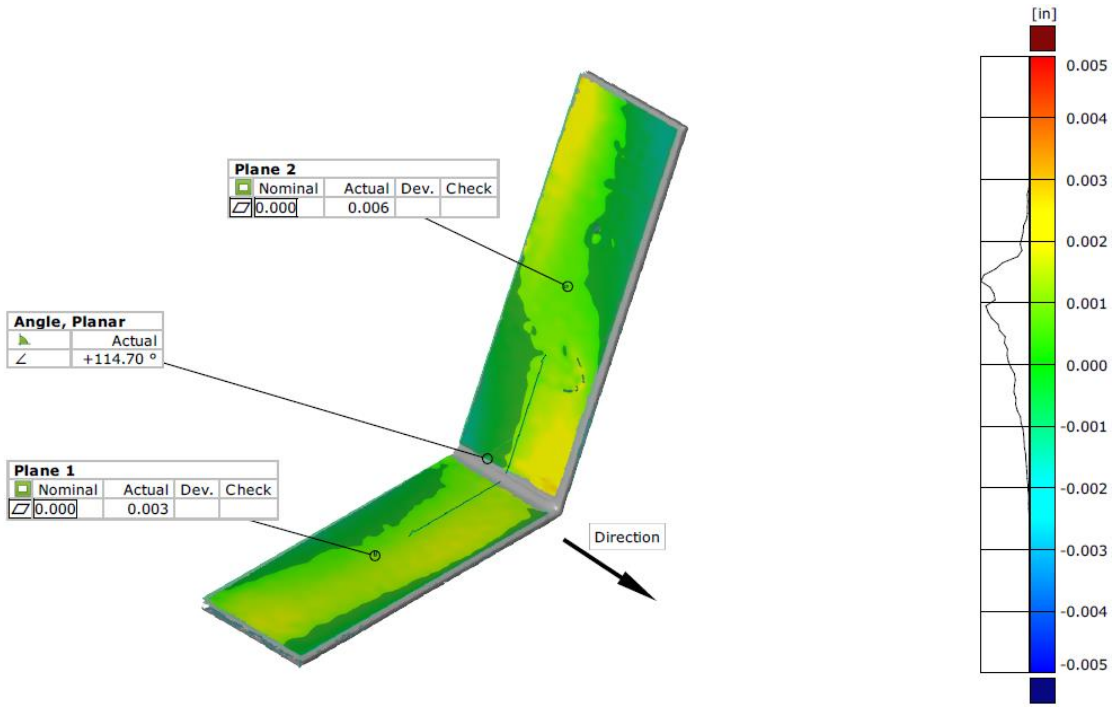

Vacuum, ambient temperature

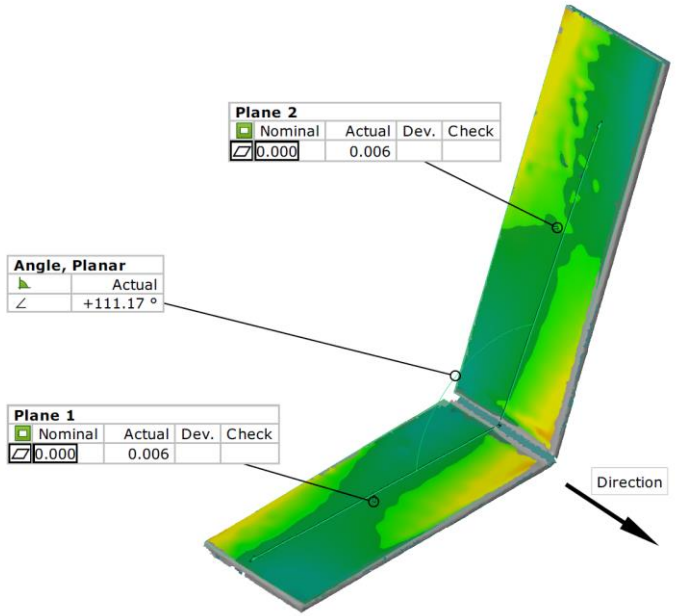

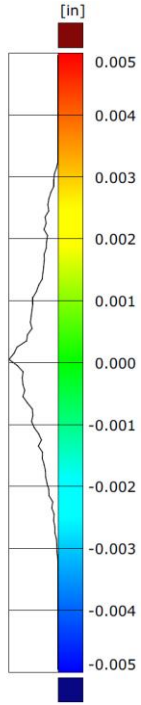

Trending towards significantly lower distortion under vacuum compared to in air

n.b. direction here is labelled opposite to actual

Progression of flight experiments

Complete
Anticipated
Notional

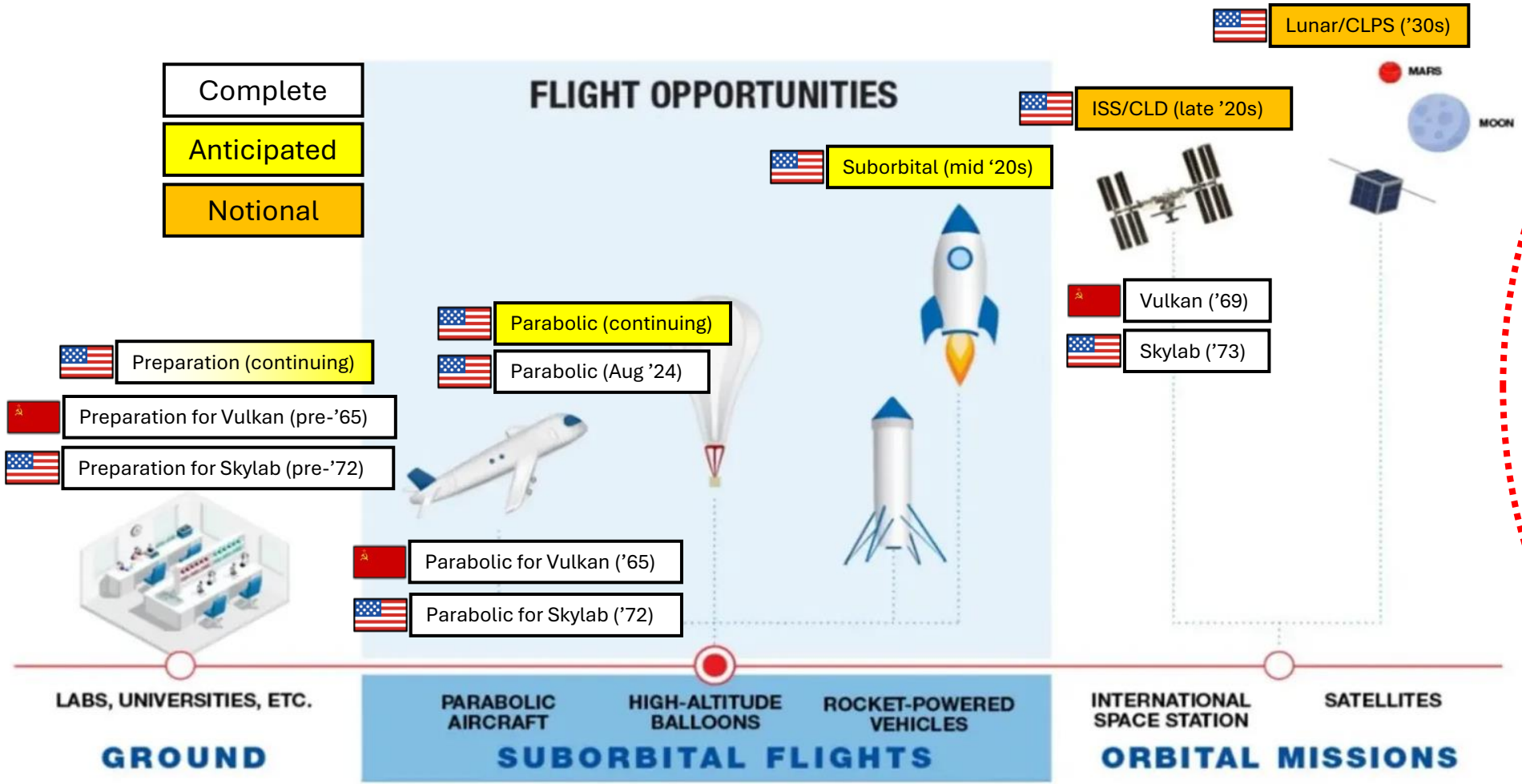

Concurrent development of Digital Twin using collected data

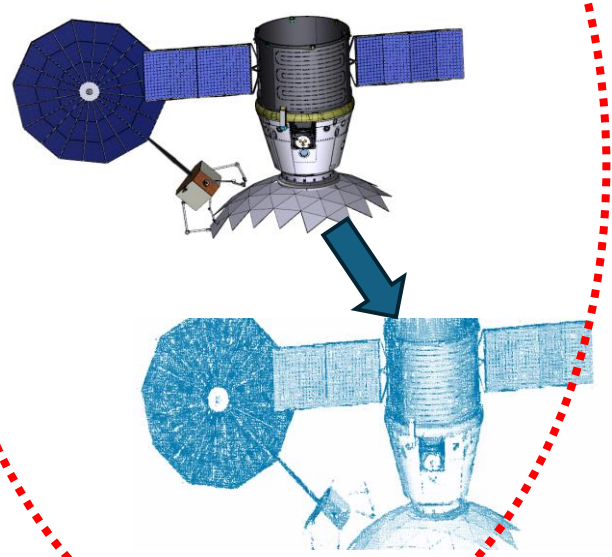

Underlying graphic from Kelly *et al.* in *ASCEND 2020*, 2020. doi: 10.2514/6.2020-4135. USG work.

Skylab Electron Beam Welds: Structure-Property-Processing

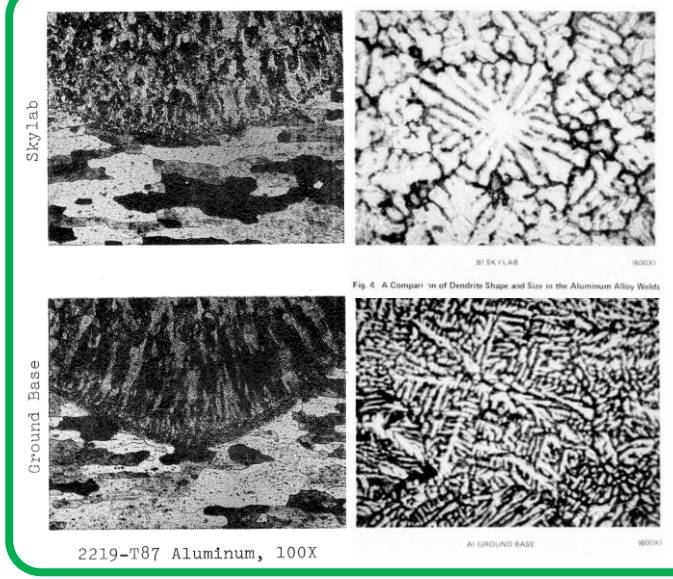

- In the ground-based samples, the dendrites are much larger at the root region than at the crown region. For Skylab samples, reduced difference in size.
- Concluded some unknown combination of ***G*** *(temperature gradient)* and ***R*** *(solidification range)* varied between ground and flight

G. Busch. Grumman Report (1976). https://ntrs.nasa.gov/citations/19770024270

Structure

Processing

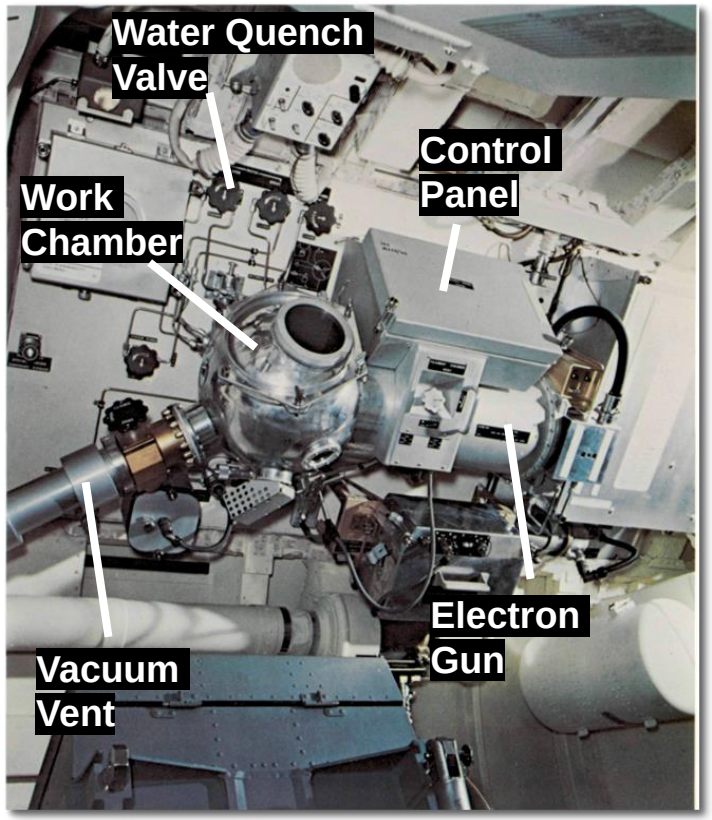

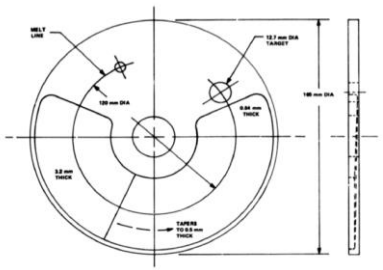

Travel speed = 1.61 cm/s, E = 20 kV, I = 50-80 mA
Alloys: Stainless Steel (304), Aluminum (2219-T87), CP Tantalum.
After 2 hr space vent, Vacuum = 10^{-4} Torr (~10^{-2} Pa)

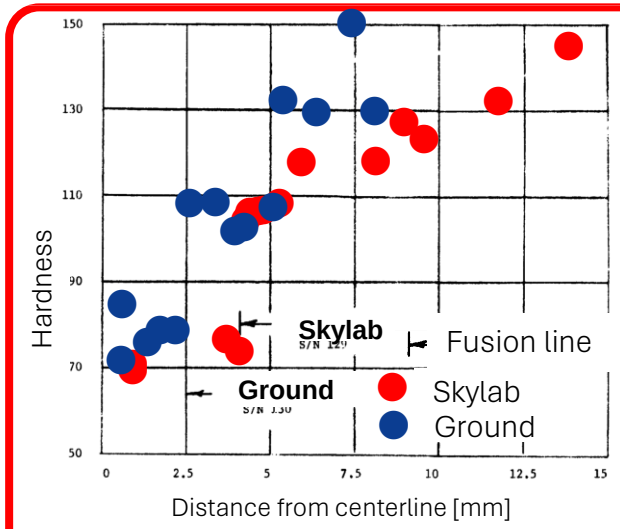

R.E. Monroe. NASA CR-129041 (1974). https://ntrs.nasa.gov/citations/19750002046

Properties

- Monroe (1974) produced hardness plots for full penetration Skylab and Ground welds.
- Li et al. (1976) concluded that no significant differences in hardness were observed between the ground-based and Skylab samples of 2219. Tantalum discs did show a significant difference, but no explanation was provided.

Computational and Physics-Based Modeling for the Development of in-Space Welding Technology - NASA Technical Reports Server (NTRS)

Temperature and gradient maps of Skylab 2219 Al disc at 100K, 293K, 400K

T_0 = 100 K	T_0 = 293 K	T_0 = 400 K
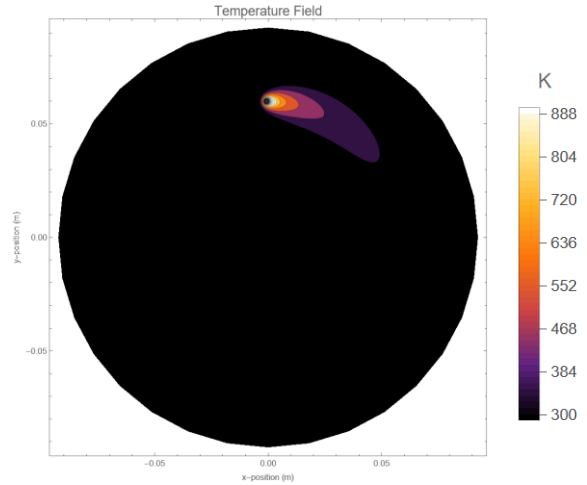	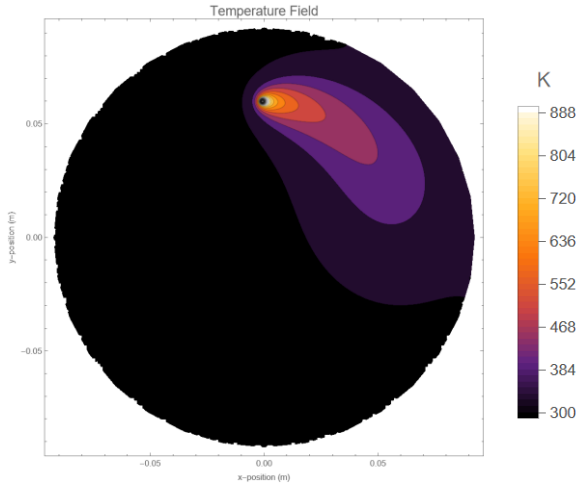	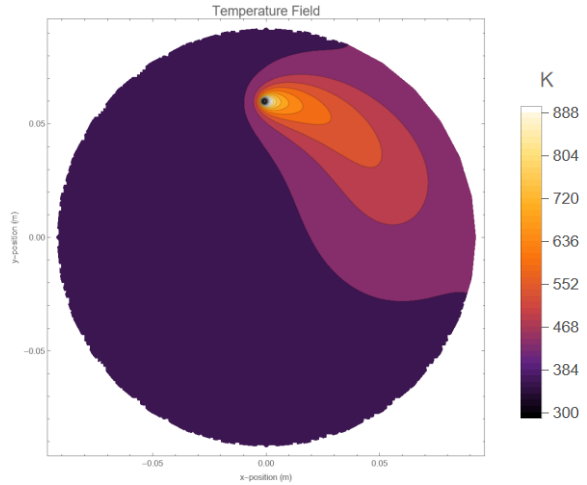
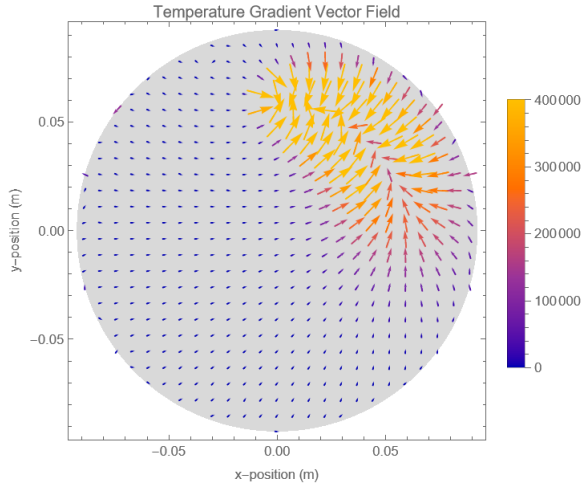	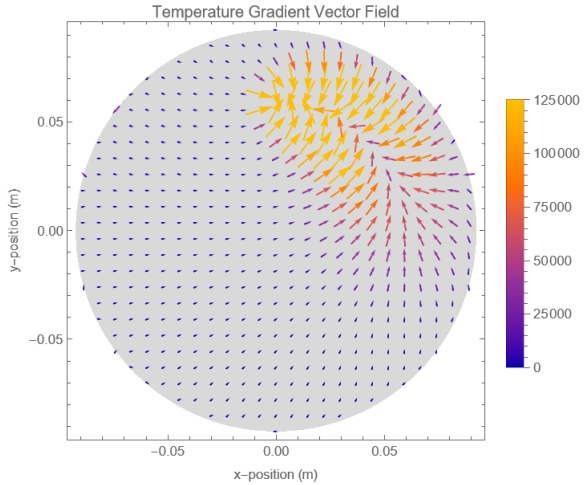	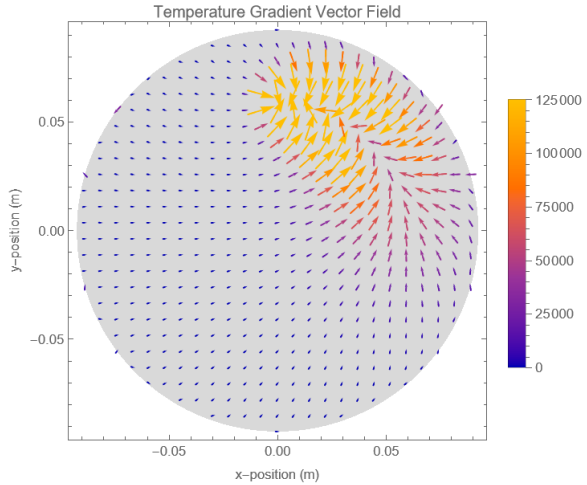

Comparison of Model and Empirical G*R

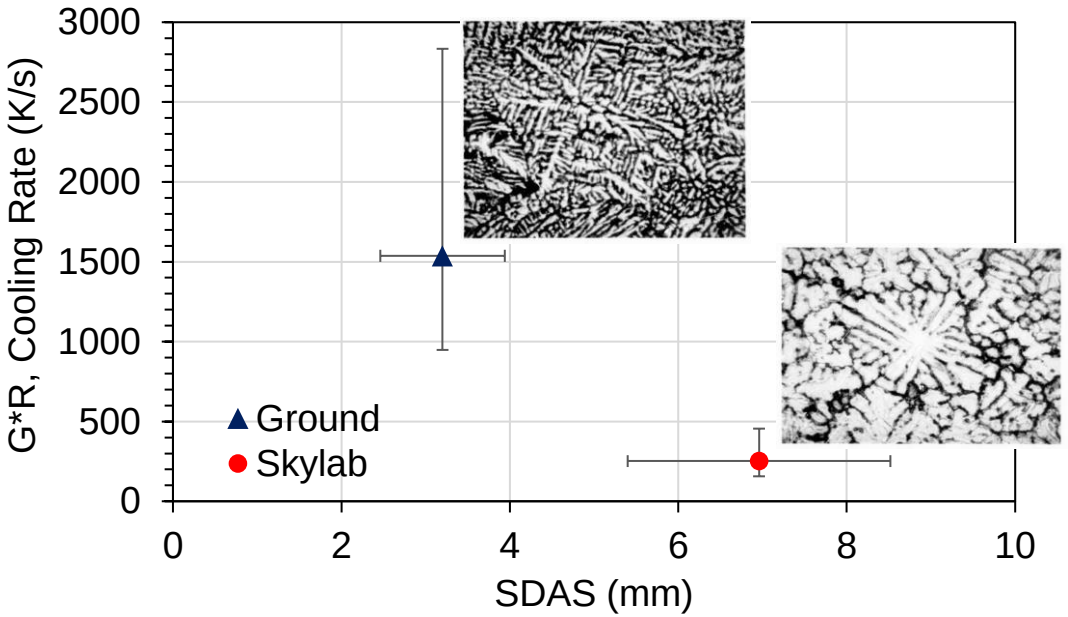

$$\lambda_2 = (143.73x^{-0.356})(G^*R)^{-0.43}$$

Brice and Dennis. *Met Trans A* 46 2015: 2304-2308.
DOI: 10.1007/s11661-015-2775-x (Wire-fed electron beam additive manufacturing process on Al-Cu)

λ_2, Secondary dendrite arm spacing (μm)
x, Cu content of AA2219 Skylab discs (6.2 wt.%)
G, Thermal gradient (K/m)
R, Growth rate (m/s) (Ground ~Travel speed = 0.015 m/s)
G*R, Cooling rate through solidification interval (K/s)

Condition	SDAS (um)	Empirical GR (K/s) from equation above	Empirical G (K/m) from equation above	R (m/s)	Macro Gradient (K/m)
Ground	3.2 +/- 0.74 (*N* = 26)	1537	$104*10^3$ K/m	0.015	$125*10^3$
Skylab	6.96 +/- 1.56 (*N* = 22)	252	$17*10^3$ K/m	Unknown due to microgravity solidification	Fluid transport neglected in model

The lack of convective currents in microgravity means heat and solute are removed from the solidification front primarily by diffusion, resulting in slower growth rates and larger dendrite arms.

Glicksman, et al. (1986). Physics Today, 39(8), 60-67. Glicksman, et al. (1992). Met Trans A, 23(4), 1531–1542.

Properties: Hardness by Starting Disc Temperature

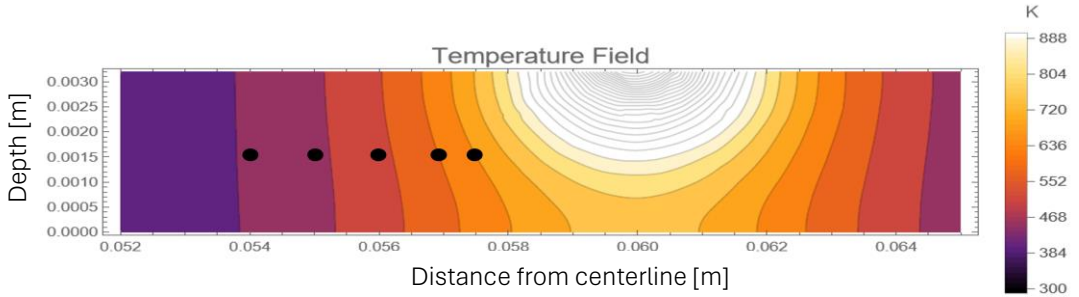

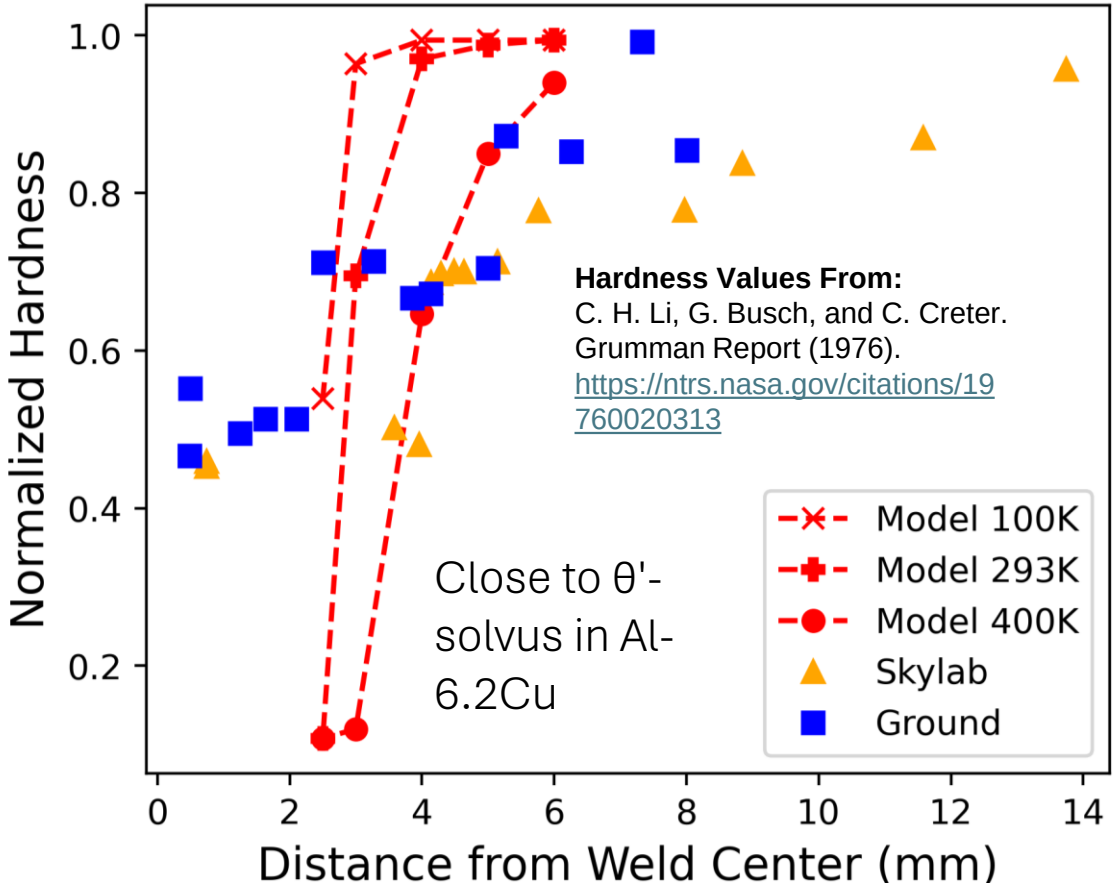

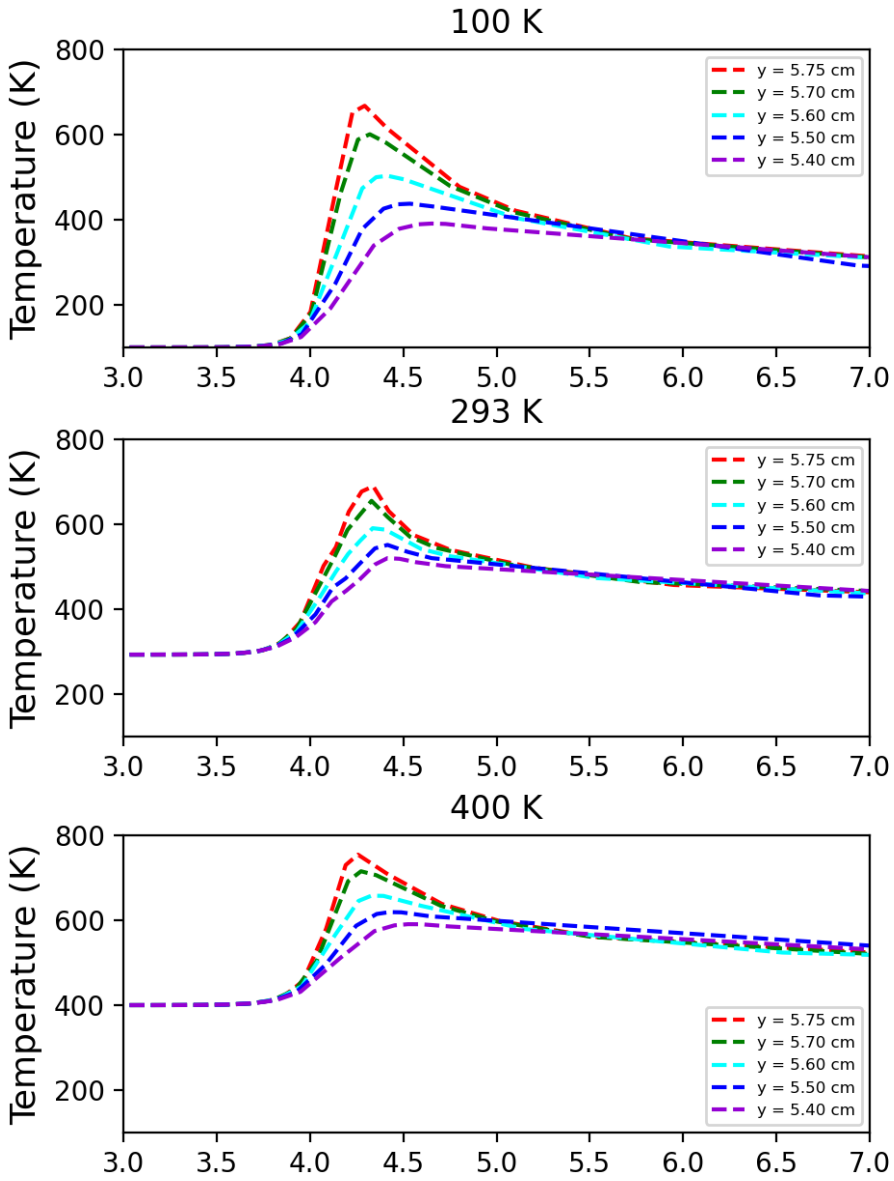

Leveraging ICME modeling to link laser absorptivity, thermophysical properties of material, laser parameters, etc.

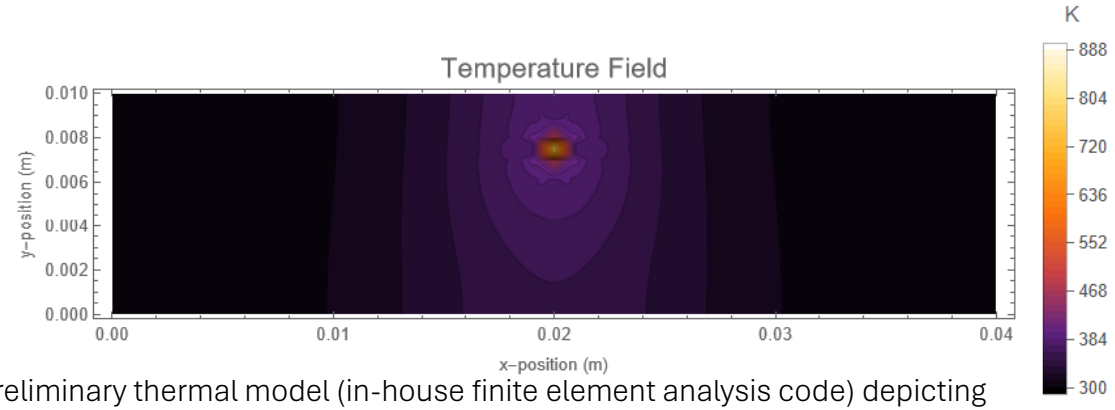

Preliminary thermal model (in-house finite element analysis code) depicting temperature field of aluminum LF coupon from above

Will validate LF and LBW thermal model with thermocouples and thermography; enhances confidence in ICME approach

To do: link thermal & thermodynamic/precipitation model to solidification, fluid flow, and grain structure

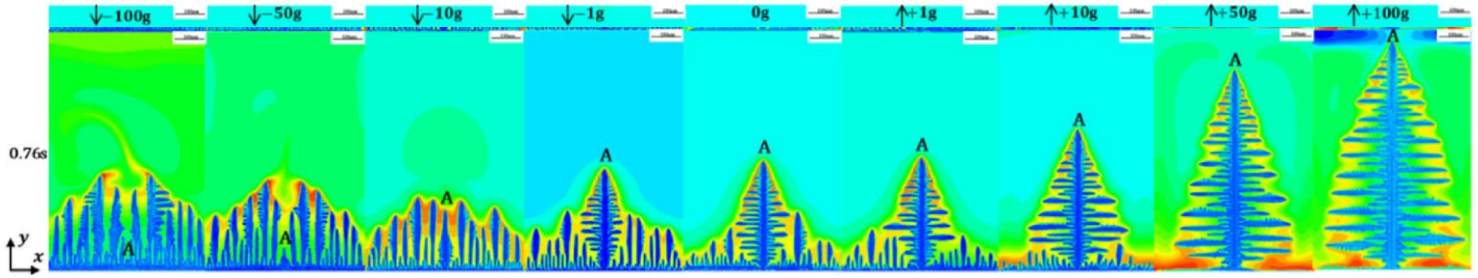

Example of a phase-field lattice-Boltzmann simulation for dendritic growth during alloy solidification in negative gravity, zero gravity, Earth-normal gravity, and hypergravity (Zhang et al., 2024, doi:10.1016/j.heliyon.2024.e27008); licensed under CC BY-NC 4.0

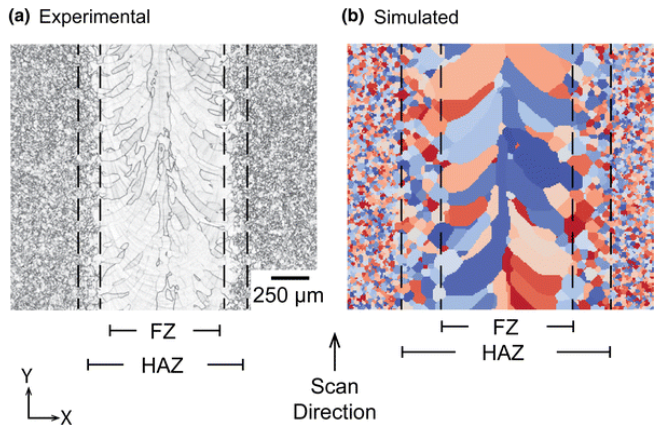

Example of a Monte Carlo Potts model in SPPARKS code to simulate grain growth in e-beam welding (Rodgers et al., 2016, doi:10.1007/s11837-016-1863-8); licensed under CC BY 4.0

Conclusions

- NASA and partners are maturing in-space welding and forming processes
- Demonstration of LBW and LF in space-like environments will enable:
  - Understand combined effects of reduced gravity, reduced pressure, varied temperatures
  - Provide validation datasets to anchor computational models
  - Mature technology to enable joining & manufacturing structures in space
- Building ecosystem of hardware, expertise, and partnering opportunities
  - Suborbital flight unit hardware
  - Parabolic and suborbital flight experiment know-how
  - TVAC experience and instrumentation expertise
  - Computational models anchored by collected data
  - Network of academic (OSU), government (AFRL, DARPA), and industrial (Laserline, Lockheed Martin, Motiv, PickNik, ThinkOrbital) partners; open to collaborations and partnerships, technology transfer, etc.

Acknowledgements

- NASA support from Marshall Space Flight Center internal funds, Biological and Physical Sciences Division of NASA Science Mission Directorate, NASA Space Technology Mission Directorate, etc.
- OSU support from Marshall Space Flight Center internal funds via
  - 80NSSC22M0209 - Integration and Demonstration of Self-contained Laser Welding System for Microgravity Experiments – NASA Cooperative Agreement Notice (CAN)
- Second parabolic flight day support from NASA Flight Opportunities